THE SIMULATION OF GAS TURBINES BY A STATE OF THE ART ANALOG DEVICE

by

WILLIAM MCMICHAEL SHEPHERD

B.S.A.E., U.S. Naval Academy
(1971)

SUBMITTED IN PARTIAL FULFILLMENT
OF THE REQUIREMENTS FOR THE
DEGREE OF
OCEAN ENGINEER
AND THE DEGREE OF
MASTER OF SCIENCE IN MECHANICAL ENGINEERING

AT THE

MASSACHUSETTS INSTITUTE OF TECHNOLOGY
May 1978

Signature of Author ....
Department of Ocean Engineering

Certified by ....
Thesis Supervisor

Certified by ....
Ocean Engineering Department Reader

Accepted by ....
Chairman, Departmental Committee on
Graduate Students

THE SIMULATION OF GAS TURBINES BY A STATE OF THE ART ANALOG DEVICE

by

William McMichael Shepherd

Submitted to the Department of Ocean Engineering on 12 May 1978 in partial fulfillment of the requirements for the Degree of Ocean Engineer and the Degree of Master of Science in Mechanical Engineering.

ABSTRACT

A simulator was designed to model the operation of a single shaft gas turbine engine. The engine characteristics were represented by a third order non linear mathematical model implemented with analog computation. The use of "state of the art" integrated circuitry allowed for a considerable reduction in the space and power required for this device compared with conventional analog methods. A hard-wired desk-top machine was fabricated to simulate the real time dynamic behavior of a gas turbine prime mover.

Thesis Supervisor: Henry M. Paynter
Title: Professor of Mechanical Engineering

Thesis Reader: A. Douglas Carmichael
Title: Professor of Power Engineering

ACKNOWLEDGEMENTS

The author wishes to acknowledge Professors H. M. Paynter and A. D. Carmichael for their assistance, advice, and guidance in the completion of this paper. Special thanks is also extended to Mr. Ken Busick of the Beede Instrument Company, and Mr. John Carter of the Henschel Corporation for providing much needed hardware.

TABLE OF CONTENTS

Page

Page

I. INTRODUCTION

A. BACKGROUND

This paper describes the concept and construction of a hard wired analog device, pictured below, which simulates the operation of a gas turbine engine.

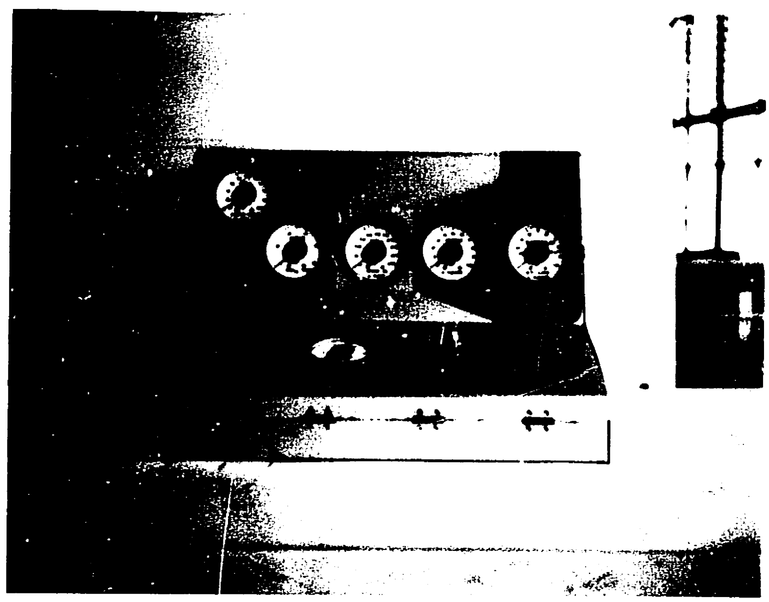

Recent work on gas turbine simulation has focused largely on digital or hybrid computing. To accommodate the nonlinear elements of a gas turbine simulation in this fashion requires a perturbation or piecewise linear technique. A pure analog approach offers a continuous

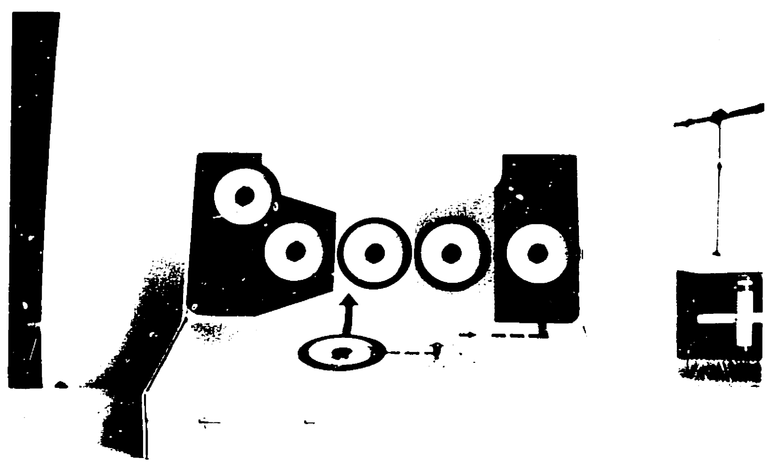

solution to these nonlinear characteristics, which facilitates a simulation in real time.

At this time, analog computation of complex nonlinear systems is not feasible on devices such as the EAI 680 computer currently installed in the M.I.T. Joint Computer Facility. With the miniaturization of both digital and linear functions into the now-common integrated circuit or IC chip, it becomes possible to design extremely compact analog devices. The IC component cost of such a simulation is rapidly approaching the cost of purely passive electronic elements.

The modeling approach to the analog simulation, physical modeling, follows the work of Markunas[1] closely. Physical modeling attempts to explain the engine characteristics within a framework of physical princples and laws which describe the functions occurring in the real machine. Simplicity is generally a strong point of the model.

The model which has been implemented in the analog simulation represents a general machine "invented" by Markunas, who estimated the necessary characteristic relations between the independent variables. Markunas conducted digital and hybrid simulations of his "general" gas turbine, but a full analog implementation was not investigated.

This paper is essentially a design manual which traces the development of a hard-wired analog simulator. It is intended to give the reader a brief overview of the analog devices currently available, and their application to a computational circuit. To facilitate future work with the simulator, a detailed user's manual has been written.

This document contains explicit details relating to the construction and operation of the simulator. The user's manual, the simulator, and associated hardware are under the supervisor of Professor Henry M. Paynter, Department of Mechanical Engineering.

B. DESIGN CONCEPT

The following characteristics were desired in the hard-wired simulator:

1. Real time, non-linear third order simulation of the dynamics of a single shaft gas turbine engine, from start-up to overload conditions.
2. Cost to be under $600.
3. Size of the device such as to be readily portable and convenient to set-up and operate.
4. Layout and operation of the simulator to be comparable with typical industrial

and military engine control consoles.

5. Accuracy of the steady-state simulation to be considered of secondary importance compared with the representation of large scale transient effects.
6. The ability to investigate various fuel control schemes in a closed loop control, and the ability to operate with different torque-speed load characteristics.
7. Utilization of the general purpose, low cost IC operational amplifier in a hard wired configuration to accomplish all mathematical operations.

II. MODELING

A. GENERAL APPROACH

The gas turbine model selected by Markunas will be briefly explained. The modeling approach is broken down into: steady state and dimensional considerations, frequency analysis, and dynamic equations.

Markunas' estimated performance parameters and the dynamic equations are combined in state-variable format. These equations appear in Appendix II and form the basis for the analog signal flow used in the design.

B. STEADY STATE AND DIMENSIONAL ANALYSIS

Horlock[3] establishes non-dimensional functions in describing the performance of compressors and turbines. A set of relations are developed to describe the performance of a turbomachine in its simplest terms.

In the subsequent development, gas turbine state points are used, numbered in the following convention, with total values indicated by a zero in front of the state point:

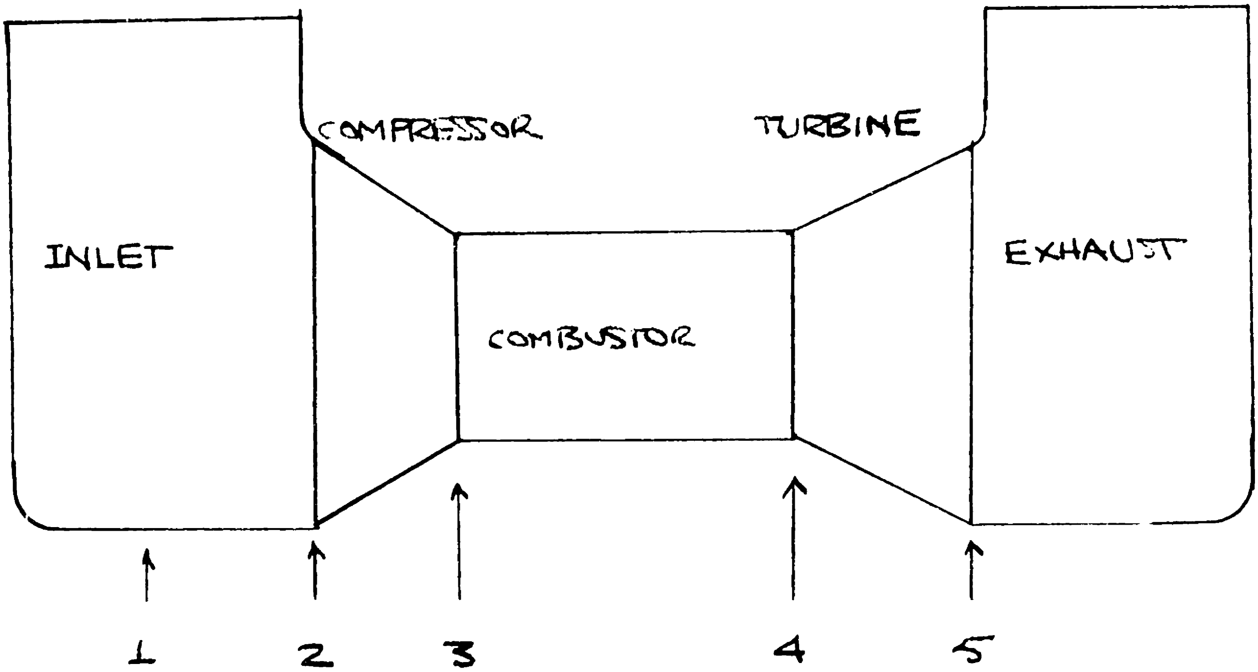

The following symbols are used for dimensional analysis in the compressor:

Symbol	Compressor	Dimensions
P_{o2}	Inlet stagnation pressure	M/LT^2
ρ_{o2}	Inlet stagnation density	M/L^3
P_{o3}	Outlet stagnation pressure	M/LT^2
T_{o2}	Inlet stagnation temperature	θ
η	Efficiency	—
D	A characteristic linear dimension	L
ΔT_o	Stagnation temperature rise through compressor	θ
N	Rotational speed	$1/T$
$\dot{m}$	Mass flow rate of gas	M/T

Symbol	Compressor	Dimensions
$\mathcal{M}$	Molecular wt of gas	—
μ	Absolute viscosity of gas	M/LT
c_p	Specific heat at constant pressure	$L^2/T^2\Theta$
γ	Ratio of specific heats	—
R	Gas constant	$L^2/T^2\Theta$
a_{02}	Speed of sound of entering gas	L/T
$\mathcal{T}_I$	Torque input	ML^2/T^2

In the compressor, if $P_{03}, \eta, \mathcal{T}_I$ and ΔT_0 are chosen as variables of interest, one can write

$$P_{03}, \eta, \mathcal{T}_I, \Delta T_0 = f\left(P_{02}, T_{02}, N, D, \dot{m}, \rho_{02}, \gamma, \mu, a_{02}\right)$$

Assuming a perfect gas, fixing the gas constant, R, choosing γ, and T_{02} thus constrains a_{02}. ρ_{02} can be expressed in terms of R, P_{02}, T_{02}; the original relation becomes

$$P_{03}, \eta, \mathcal{T}_I, \Delta T_0 = f\left(P_{02}, T_{02}, N, D, \dot{m}, R, \gamma, \mu\right)$$

Taking non-dimensional groups,

$$\frac{P_{03}}{P_{02}}, \eta, \frac{\mathcal{T}_I}{P_{02}D^3}, \frac{\Delta T_0}{T_{02}} = f\left(\frac{ND}{R\sqrt{T_{02}}}, \frac{\dot{m}\sqrt{RT_{02}}}{P_{02}D^2}, \frac{P_{02}D}{\mu\sqrt{T_{02}}}, \gamma\right)$$

With constant values, R and γ can be eliminated:

$$\frac{P_{03}}{P_{02}}, \eta, \frac{\mathcal{T}_I}{P_{02}D^3}, \frac{\Delta T_0}{T_{02}} = f\left(\frac{ND}{\sqrt{T_{02}}}, \frac{\dot{m}\sqrt{T_{02}}}{P_{02}D^2}, \frac{P_{02}D}{\mu\sqrt{T_{02}}}\right)$$

Multiplying the last two non-dimensional parameters to create a new parameter,

$$\frac{P_{o3}}{P_{o2}}, \eta, \frac{\tau_1}{P_{o2}D^3}, \frac{\Delta T_o}{T_{o2}} = f\left(\frac{ND}{\sqrt{T_{o2}}}, \frac{\dot{m}\sqrt{T_{o2}}}{P_{o2}D^2}, \frac{\dot{m}}{\mu D}\right)$$

It can be seen that the third parameter, $\frac{\dot{m}}{\mu D}$ is a "flow Reynolds number".

Assuming that the compressor operates above some critical Reynolds number, and that the dimensions of a particular machine are fixed, the equations reduce to:

$$\frac{P_{o3}}{P_{o2}}, \eta, \frac{\tau_1}{P_{o2}}, \frac{\Delta T_o}{T_{o2}} = f\left(\frac{N}{\sqrt{T_{o2}}}, \frac{\dot{m}\sqrt{T_{o2}}}{P_{o2}}\right)$$

In order to present meaningful performance relations, compressor data should be corrected following the above parameters.

Identically for a turbine,[4] it can be shown that the same relations hold and that the parameters of interest in turbine performance[3] are $\dot{m}, \eta, \tau_2, \Delta T_o$. All inlet conditions assume values at state point 4, and all exit values are at state point 5. Torque across the turbine is τ_2. As shown before,

$$\frac{\dot{m}\sqrt{T_{o4}}}{P_{o4}}, \eta, \frac{\tau_2}{P_{o4}}, \frac{\Delta T_o}{T_{o4}} = f\left(\frac{N}{\sqrt{T_{o4}}}, \frac{P_{o5}}{P_{o4}}\right)$$

The characteristics for a given turbomachine can now be specified as functions of dimensionless or pseudo-dimensionless groups:

Compressor:

$$\frac{\dot{m}\sqrt{T_{o2}}}{P_{o2}} = f\left(\frac{P_{o3}}{P_{o2}}, \frac{N}{\sqrt{T_{o2}}}\right)$$

$$\frac{T_{o3}}{T_{o2}} = f\left(\frac{P_{o3}}{P_{o2}}, \frac{N}{\sqrt{T_{o2}}}\right)$$

$$\frac{\tau_1}{P_{o2}} = f\left(\frac{P_{o3}}{P_{o2}}, \frac{N}{\sqrt{T_{o2}}}\right)$$

Turbine:

$$\frac{\dot{m}\sqrt{T_{o4}}}{P_{o4}} = f\left(\frac{P_{o5}}{P_{o4}}, \frac{N}{\sqrt{T_{o4}}}\right)$$

$$\frac{T_{o5}}{T_{o4}} = f\left(\frac{P_{o5}}{P_{o4}}, \frac{N}{\sqrt{T_{o4}}}\right)$$

$$\frac{\tau_2}{P_{o4}} = f\left(\frac{P_{o5}}{P_{o4}}, \frac{N}{\sqrt{T_{o4}}}\right)$$

C. FREQUENCY ANALYSIS

Modeling of the processes which take place in a gas turbine can generally be classified as mechanical, fluid, or thermal in nature. To reduce the scope of the problem to a more manageable field, only the most significant energy domains and dynamics were considered. Markunas defines three dynamic regimes for the gas turbine:

1. Low frequency, ($f \approx .1$ hz) where rotary inertias and thermal capacitances dominate the dynamics.
2. Medium frequency ($f \approx 1$ hz) where rotary inertias and fluid capacitances dominate.
3. High frequency ($f \gtrsim 100$ hz) where the fluid dynamics are dominant.

Markunas established that rotor dynamics and fluid capacitances were the primary influences on gas turbine dynamics. Thermal capacitances and fluid inertias were neglected.

D. DYNAMIC EQUATIONS

1. Assumptions

The gas turbine model is assumed to operate with a perfect gas in one-dimensional flow. Components are treated in lumped parameter fashion.

2. Rotor Inertia

For the rotor, a summation of torques give the following:

$$\dot{N}_G = \frac{30}{\pi I_R} \sum \tau$$

where

$\dot{N}_G$ = angular acceleration, rpm/sec

I_R = rotary inertia, ft-lbf-sec^2

τ = load, compressor, or turbine torque, ft-lbf

3. Fluid Capacitance

For the one-dimensional lumped parameter fluid, the following symbology is used:

ρ = fluid density, lbm/ft^3

x = axial distance along duct, ft

V_x = mean axial velocity of fluid, ft/sec

γ = ratio of specific heats = C_p/C_v

C_p = specific heat at constant pressure

C_v = specific heat at constant volume

M = Mach number = V_x/a

a = Local sonic velocity = $\sqrt{g_c \gamma R T}$

u = internal energy of the fluid in ft-lbf/lbm

h = enthalpy of the fluid in ft-lbf/lbm

VOL = lumped fluid volume

A general mass conservation equation for the one dimensional fluid stream may be written:

$$\frac{\partial(\rho)}{\partial t} + \frac{\partial}{\partial x}(\rho V_x) = 0$$

Integrating over a constant area duct, with fluid properties constant at a given axial distance or dimension:

$$\frac{\partial}{\partial t}(\rho A) + \frac{\partial}{\partial x}(\rho A V_x) = 0$$

$$\frac{\partial A}{\partial x} \equiv 0 \qquad \text{by definition.}$$

Integrating over the length of the duct

$$\frac{\partial}{\partial t}\int_L \rho A\, dx + \int_L \frac{\partial}{\partial x}(\rho A V_x)\, dx = 0$$

$$\frac{\partial}{\partial t}(\bar{\rho} \cdot VOL) + \rho A V_x \Big|_0^L = 0$$

$\int_L \rho A\, dx$ is approximated by an average density, $\bar{\rho}$. Lumped fluid volume (VOL) since

$$\frac{d}{dt}(\bar{\rho}) = \frac{1}{VOL}(\dot{m}_1 - \dot{m}_2)$$

where the subscipts 1 and 2 identify inlet and outlet conditions across the engine, respectively.

Writing a similar equation for the conservation of momentum neglecting viscous shear and body forces,

$$\frac{\partial}{\partial t}\left(\frac{\rho V_x}{g_c}\right) + \frac{\partial}{\partial x}\left(\frac{\rho V_x^2}{g_c} + P\right) = 0$$

Integrating over area,

$$\frac{\partial}{\partial t}\left(\frac{\rho V_x A}{g_c}\right) + \frac{\partial}{\partial x}\left(\frac{\rho V_x^2 A}{g_c} + PA\right) = 0$$

$$\frac{\partial}{\partial t}\left(\frac{\rho V_x A}{g_c}\right) + \frac{\partial}{\partial x}\left(\frac{\rho V_x^2 A}{g_c}\right) + \frac{\partial}{\partial x}(PA) = 0$$

$$\frac{\partial}{\partial t}\left(\frac{\rho V_x A}{g_c}\right) + \frac{V_x^2}{g_c} A \frac{\partial \rho}{\partial x} + A\frac{\partial}{\partial x}(P) = 0$$

Integrating over length of the duct

$$\frac{\partial}{\partial t}\int_L \left(\frac{\rho V_x A}{g_c}\right) dx + \left.\frac{\rho V_x^2 A}{g_c}\right|_1^2 + \left. PA\right|_1^2 = 0$$

$$\frac{\partial}{\partial t}\int_L \frac{\dot{m}}{g_c}\, dx + \left[\frac{\rho V_x^2 A}{g_c} + PA\right]_1^2 = 0$$

$$\frac{d}{dt}\left(\frac{\bar{\dot{m}} L}{g_c}\right) = \left[PA + \frac{\rho V_x^2 A}{g_c}\right]_2^1$$

$$\frac{d}{dt}\left(\bar{\dot{m}}\right) = \frac{g_c A}{L}\left[P + \frac{\rho V_x^2}{g_c}\right]_2^1$$

$\bar{\dot{m}} \equiv$ AVERAGE VALUE

$$M^2 = \frac{V_x^2}{a^2} = \frac{V_x^2}{g_c \gamma R T}$$

$$\frac{d}{dt}(\bar{\dot{m}}) = \left[\frac{g_c A}{L}\right]\left[P(1 + \gamma M^2)\right]_2^1$$

Since total pressure, $P_0 \equiv P\left(1 + \frac{\gamma - 1}{2} M^2\right)^{\frac{\gamma}{\gamma - 1}}$

$$\frac{d}{dt}(\bar{\dot{m}}) = \left[\frac{g_c A}{L}\right]\left[\frac{P_0 (1 + \gamma M^2)}{\left(1 + \frac{\gamma - 1}{2} M^2\right)^{\gamma/\gamma - 1}}\right]_2^1$$

Assuming $\gamma = 1.4$, and $M \leq .5$, the momentum equation can be written:

$$\frac{d}{dt}(\bar{\dot{m}}) \cong \frac{g_c A}{L}(P_{o1} - P_{o2})$$

Similarly for energy conservation with no external work or heat addition,

$$\frac{\partial}{\partial t}\left[\rho\left(u + \frac{V_x^2}{2g_c}\right)\right] + \frac{\partial}{\partial x}\left[\rho V_x\left(h + \frac{V_x^2}{2g_c}\right)\right] = 0$$

Integrating over area and length,

$$\frac{\partial}{\partial t}\int_0^L \left[\rho A\left(u + \frac{V_x^2}{2g_c}\right)\right] dx + \dot{m}\left(h + \frac{V_x^2}{2g_c}\right)\Bigg|_1^2 = 0$$

$$(VOL)\frac{d}{dt}\left[\rho\left(u+\frac{V_x^2}{2g_c}\right)\right] = \dot{m}h_o\Big|_2^1$$

where

$$h_o \equiv h + \frac{V_x^2}{2g_c}$$

Since

$$\frac{V_x^2}{2g_c} = \frac{\gamma RT M^2}{2}$$

Substituting,

$$u + \frac{V_x^2}{2g_c} = c_vT\left(1 + \frac{\gamma(\gamma-1)}{2}M^2\right)$$

$$\frac{d}{dt}\left[\left(\overline{\rho c_v T_o}\right)\frac{1+\frac{\gamma(\gamma-1)}{2}M^2}{1+\frac{\gamma-1}{2}M^2}\right] = \frac{c_p}{VOL}\left(\dot{m}_1T_{o1} - \dot{m}_2T_{o2}\right)$$

where $T_o = T + \left(1 + \frac{\gamma-1}{2}M^2\right)$

With $M \leq .5$ the result can be simplified to:

$$\frac{d}{dt}\left(\overline{\rho T_o}\right) = \frac{\gamma}{Vol}\left(\dot{m}_1 T_{o1} - \dot{m}_2 T_{o2}\right)$$

E. STATE EQUATIONS

The three conservation equations are now:

1. Mass

$$\frac{d}{dt}(\bar{\rho}) = \frac{1}{VOL}\left(\dot{m}_1 - \dot{m}_2\right)$$

2. Momentum

$$\frac{d}{dt}(\bar{\dot{m}}) = \frac{g_c A}{L}(P_{o1} - P_{o2})$$

3. Energy

$$\frac{d}{dt}(\overline{\rho T_o}) = \frac{\gamma}{VOL}(\dot{m}_1 T_{o1} - \dot{m}_2 T_{o2})$$

Using the definition of a polytropic process, $PV^n = \text{CONST}$, it follows that

$$P_o = (\text{CONST})\,\rho_o^{\,n}$$

$$T_o = (\text{CONST})\,P_o^{\frac{n-1}{n}} = (\text{CONST})\,\rho_o^{\,n-1}$$

In order to get the mass and energy equations into more convenient form,

$$\frac{d}{dt}(P_o) = (\text{CONST})(n)\frac{d}{dt}(\rho_o)$$

$$\frac{d}{dt}(\rho_o) = \left(\frac{1}{nRT_o}\right)\frac{d}{dt}(P_o)$$

$$\frac{d}{dt}(\rho_o T_o) = \text{CONST}\,\rho_o^{\,n}\frac{dT_o}{dt} + (n-1)\,\text{CONST}\,\frac{d\rho_o}{dt}T_o$$

$$\frac{d}{dt}(\rho_o T_o) = \left(\frac{n}{n-1}\right)\left(\frac{P_o}{RT_o}\right)\frac{d}{dt}(T_o)$$

(WHERE $\bar{\rho}$ IS ASSUMED TO TAKE STAGNATION VALUES)

With the result that the equations now be more:

$$\frac{d}{dt}(\overline{P_0}) = \frac{n R \overline{T_0}}{VOL}(\dot{m}_1 - \dot{m}_2)$$

$$\frac{d}{dt}(\dot{m}) = \frac{\overline{g_c A}}{L}(P_{01} - P_{02})$$

$$\frac{d}{dt}(\overline{T_0}) = \frac{n-1}{n}\left(\frac{C_p R \overline{T_0}}{C_v \overline{P_0}\, VOL}\right)(\dot{m}_1 T_{01} - \dot{m}_2 T_{02})$$

Where 1 and 2 represent inlet and outlet across the duct. Because of lumped parameter considerations, machine model parameters can be substituted as follows:

One Dimensional	Machine Model
$\dot{m}_1$	$\dot{m}_3$
$\dot{m}_2$	$\dot{m}_4$
$\overline{T_0}$	T_{04}
T_{01}	T_{03}
T_{02}	T_{04}
$\overline{P_0}$	P_{03}

Substituting notation for the first and third differential equations,

$$\dot{P}_{03} = \left(\frac{n R \overline{T_{04}}}{VOL}\right)\left[\dot{m}_3 - \dot{m}_4\right]$$

$$\dot{T}_{o4} = \left(\frac{n-1}{n}\,\frac{\gamma R T_{o4}}{P_{o3}\,VOL}\right)\left[\dot{m}_3 T_{o3} + \dot{m}_F\left(\frac{h_{LHV}}{c_p}\right) - \dot{m}_4 T_{o4}\right]$$

Introducing the torque equation as the third system equation,

$$\dot{N}_G = \left(\frac{30}{\pi I}\right)\left[\tau_2 - \tau_L - \tau_3\right]$$

where

h_{LHV} = fuel lower heating value, Btu/lbm

$\dot{m}_F$ = fuel flow, lbm/sec

τ_3 = load torque, ft-lbf

P_{o3}, T_{o4}, AND N_G are chosen as variables of convenience.

For an isentropic process, n = 1.4. Markunas felt that n-1/n should be replaced by 1.0 in the temperature equation.

F. ENGINE DATA, ASSUMPTIONS, AND CHARACTERISTICS

1. Introduction

In Markunas' analysis a single shaft machine was invented from a number of sources. Several real world machines exist which have design parameters close to

Markunas's engine. The recent Garrett GTPF 990 engine in its locked shaft mode is a reasonable example.

2. Design Point Specifications

Pressure Ratio	5.0
Compressor Isentropic Efficiency	1280^{o}F
Turbine Isentropic Efficiency	88%
Compressor Discharge Mass Flow	100 lbm/sec
Inlet Pressure	14.175 psia
Inlet Temperature	80^{o}F
Rotor Speed	7200 rpm
Output	6948 HP

Markunas plotted characteristic curves for his compressor and turbine, which appear in Appendix I. Markunas then mathematically "fit" each characteristic curve. These approximations follow the functional relations established for non-dimensional and pseudo dimensionless groups.

3. Compressor and Turbine Characteristics

Markunas defined the following variables and characteristics for his compressor:

$PRC = P_{o3}/P_{o2}$ pressure ratio

$$TRC = T_{03}/T_{02}$$ temperature ratio

$$XWC = \frac{\dot{m}_3\sqrt{T_{02}}}{P_{02}} \Bigg/ \left(\frac{\dot{m}_3\sqrt{T_{02}}}{P_{02}}\right)_{DESIGN}$$ scaled compressor mass flow

$$XNC = \frac{N_G}{\sqrt{T_{02}}} \Bigg/ \left(\frac{N_G}{\sqrt{T_{02}}}\right)_{DESIGN}$$ scaled compressor speed

$$XMC = \frac{P_{02}}{\sqrt{T_{02}}}\left(\frac{\dot{m}_3\sqrt{T_{02}}}{P_{02}}\right)_{DESIGN}$$

$$AC = .75\,(XNC) + .27\,(XNC)^3$$

$$BC = 3.0\,(XNC)^{1.5} + 3.0\,(XNC)^7$$

$$CC = .018\,(2 - XNC)^{5.8}$$

$$DC = .891\sqrt{.9 - (XNC - .9)^2}$$

$$EC = 1.0 + XNC + 3.6\,(XNC)^{4.1}$$

$$FC = \begin{cases} 4.0 & \text{IF } PRC \le EC \\ 2.0 & \text{IF } PRC > EC \end{cases}$$

$$GEC = \frac{\gamma - 1}{\gamma}$$

$$XWC = AC\left[1 - \left(\frac{PRC - 1}{BC}\right)\right]^{CC}$$

$$EFFC = DC\left[1 - \left(\frac{EC - PRC}{EC - 1}\right)^{FC}\right]$$

$$TRC = 1 + \left[\frac{(PRC)^{GEC} - 1}{EFFC}\right]$$

Similarly, for the turbine

$$PRT = P_{05}/P_{04}$$

$$TRT = T_{05}/T_{04}$$

$$XWT = \frac{\dot{m}_4\sqrt{T_{04}}}{P_{04}} \Bigg/ \left(\frac{\dot{m}_4\sqrt{T_{04}}}{P_{04}}\right)_{DESIGN}$$

$$XMT = \frac{P_{03}}{\sqrt{T_{04}}}\left(\frac{\dot{m}_4\sqrt{T_{04}}}{P_{03}}\right)_{DESIGN}$$

$$XNT = \frac{N_G}{\sqrt{T_{04}}} \Bigg/ \left(\frac{N_G}{\sqrt{T_{04}}}\right)_{DESIGN}$$

$$AT = 1.0006$$

$$BT = 3.1 + \left(\frac{1.62}{XNT + .26}\right)$$

$$CT = .7$$

$$DT = .88\left[1 - (1 - XNT)^4\right]^{.65}$$

$$ET = 1. - .8(XNT)^{1.25}$$

$$GET = \frac{\gamma - 1}{\gamma}$$

$$XWT = AT\left[1 - (PRT)^{BT}\right]^{CT}$$

$$EFFT = 1 - \left[1 - \sqrt{\frac{1 - ET}{1 - PRT}}\right]^2$$

$$TRT = 1 - EFFT\left[1 - (PRT)^{GET}\right]$$

Additional Machine Assumptions

1. $P_{o5} = P_{o2} = P_{o1}$ (no duct loss)

$P_{o3} = P_{o4}$ (no combustor losses)

The machine characteristics are combined with the differential equations to produce a set of system state equations. The expanded equations appear in Appendix II.

III. THE OPERATIONAL AMPLIFIER

A. INTRODUCTION

The fundamentals of the operational amplifier, (OA) are briefly presented to establish the necessary analog "tools" to proceed to a simulator design.

B. BASIC OPERATION

An ideal OP amp can be modeled by the following sketch:

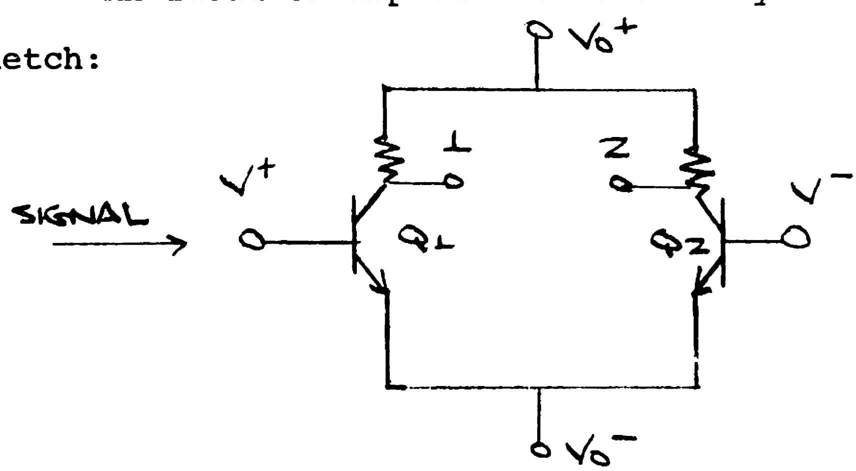

with no differential voltage between positive (V^+) and negative (V^-) inputs, both emitters are equally biased, and collector currents Q_1 and Q_2 are equal. The differential voltage output between 1 and 2 is also zero. Driving V^+ more positive with a signal will cause the current through Q_1 to increase. The current through Q_2 must decrease by a proportional amount, so that in the differential voltage output between 1 and 2, 1 gets driven more negative with respect to its initial voltage, and 2 becomes more positive.

Thus for a small signal applied to one of the input terminals, a high voltage gain and current "buffering" takes place as a result of the transistor characteristics.

With the ideal OA, the input current is essentially zero, and the voltage gain is assumed infinite.

C. THE INVERTING OA

Looking at the following diagram,

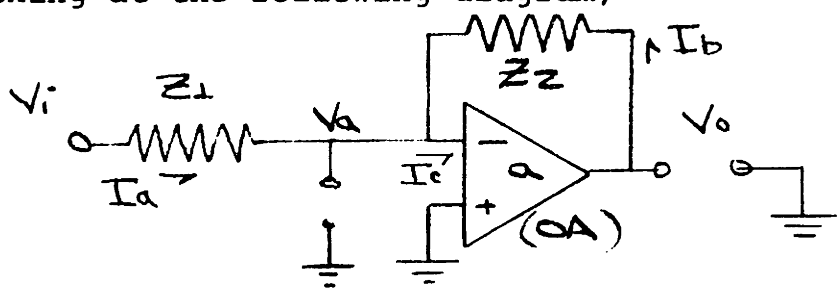

It is assumed that the impedance of the amplifier $Z_c \rightarrow \infty$, therefore $I_c \cong 0$.

Closed Loop Gain, from a summation of currents:

$$I_b = (V_o - V_a)/Z_2$$

$$I_a = (V_i - V_a)/Z_1 \; ; \; I_a \cong -I_b$$

$$-V_o/Z_2 + V_a/Z_2 = V_i/Z_1 - V_a/Z_1$$

$$\frac{V_o}{V_i} = \frac{-a Z_2/(Z_1 + Z_2)}{1 + \left[a Z_1/(Z_1 + Z_2)\right]}$$

If a, the amplifier gain, is large,

$$\frac{V_o}{V_i} \cong -\frac{Z_2}{Z_1}$$

It can therefore be seen that the inverting OA inverts and provides a gain proportional to the input and the signal feedback resistances.

D. INVERTING SUMMER

By joining multiple input currents to the input side of the OA, an inverting summer can be constructed with variable gains on each input.

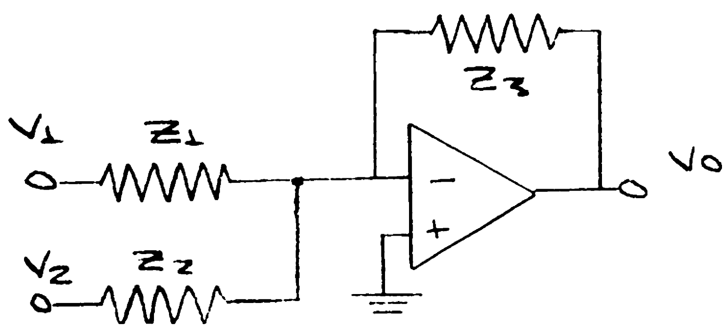

By current summation,

$$V_o/Z_3 = -V_1/Z_1 - V_2/Z_2$$

$$V_o = -V_1\frac{Z_3}{Z_1} - V_2\frac{Z_3}{Z_2}$$

E. INTEGRATOR

Adding a capacitor to the feed back loop of the OA adds the following constitutive relation to the feedback loop:

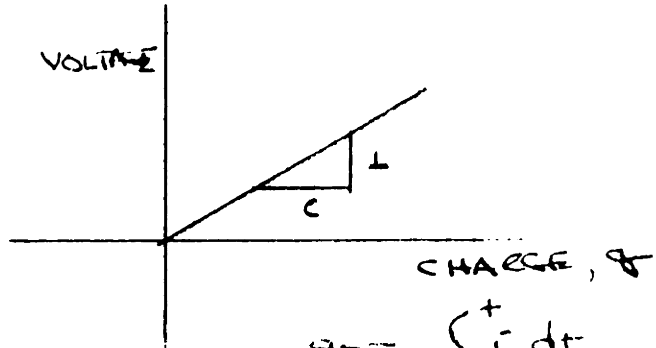

$$q = \int^{t} i \, dt$$

Looking at a typical circuit,

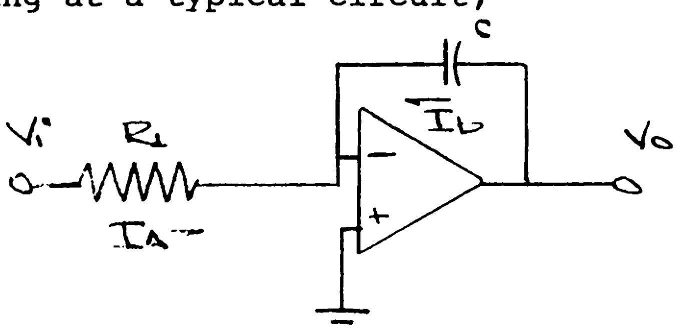

$$I_A = -I_b$$

$$\frac{\Delta V_o}{\Delta t} = \frac{I_b}{C}$$

$$\Delta V_o = -\frac{V_i}{R_1 C} \Delta t$$

$$V_o = \frac{-1}{R_1 C} \int_0^t V_i \, dt$$

F. LOGARITHMIC GENERATOR

Using a diode in the feedback loop enables the logarithmic nature of the diode voltage - current relation to be included in the loop. The diode characteristic can be modeled by the following equation:

$$\frac{I}{I_0} = \exp\left(\frac{V}{V_0}\right) - 1$$

$$\frac{V}{V_0} = \ln\left[1 + \frac{I}{I_0}\right]$$

$$V = V_0 \ln\left(I_0 + I\right)$$

where:

I_0	=	junction saturation current
V_0	=	junction saturation voltage
I	=	bias current
V	=	bias voltage

A typical characteristic appears as:

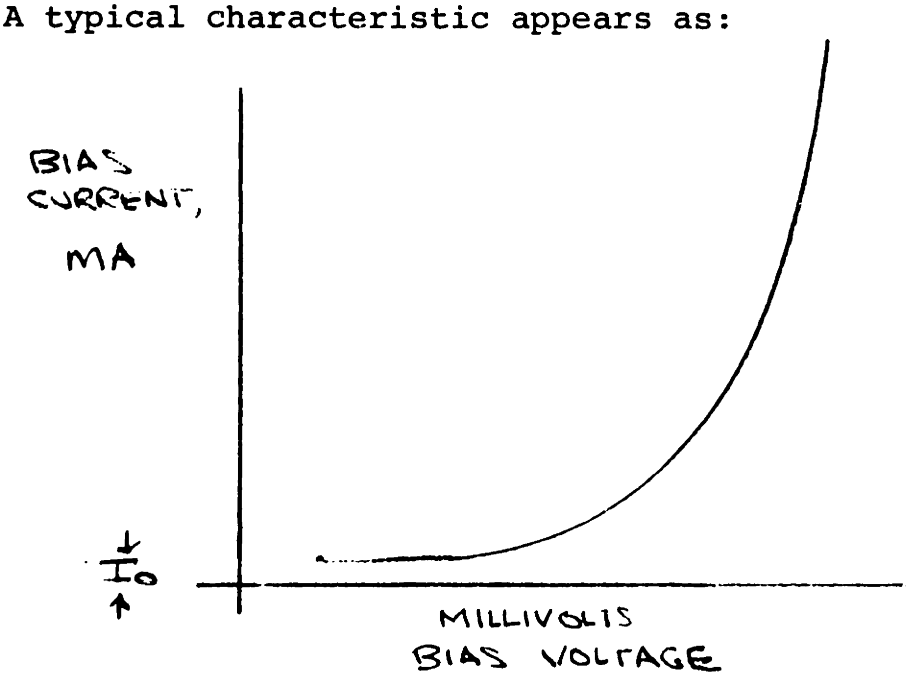

It is important to note that the saturation voltage V_o is directly proportional to the absolute temperature.

A typical log circuit can be constructed as follows:

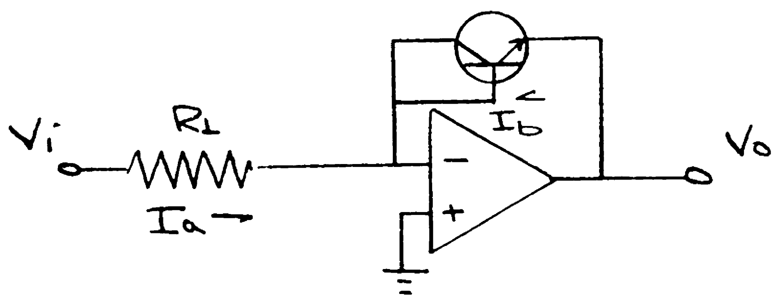

A diode - connected transistor is used to perform the diode function, as transistor emitter-base junctions have more dynamic current range than diodes in general. By the following diagram, an input V_i across R_L causes a current flow through the "transdiode". The bias voltage, appearing as V_o, varies as the log of V_i.

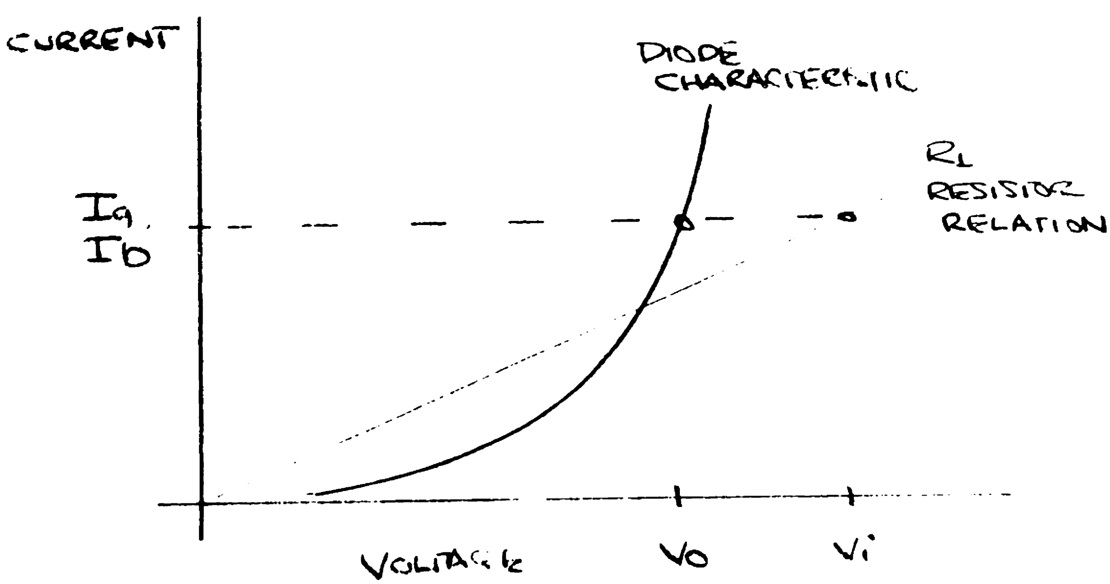

G. ANTILOG GENERATOR

In a similar fashion, input voltages or currents may be exponentiated in the following circuit:

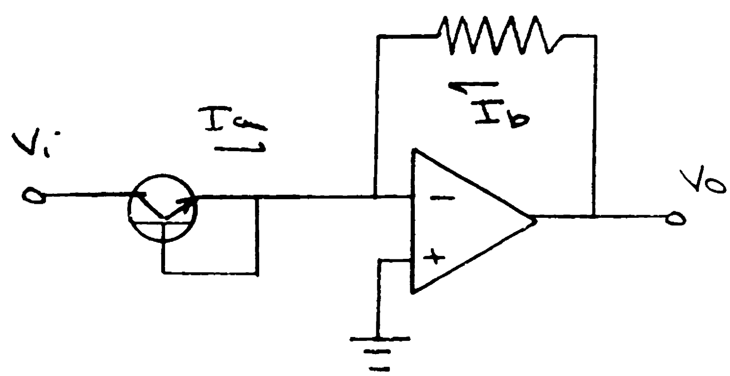

IV. ANALOG COMPUTATION

A. INTRODUCTION

To implement the non-linear system equations the following functional operations are performed: addition, subtraction, integration, multiplication, division, exponentiation to a fixed power, and exponentiation to a variable power. The first three analog operations have been briefly discussed. To implement the higher functions, the use of logarithmic circuits must be made.

B. THE PRACTICAL LOG CIRCUIT

There are at least three major considerations in the construction of a practical log or antilog circuit: cost, complexity, and accuracy. Three different architectures are considered to accomplish the log function.

The first choice is the previously discussed simple log/antilog circuit. Using low quality components, cost of the log circuit is under one dollar. Thermal stability is considered poor. A test circuit and transdiode characteristics are shown in Appendix III. Test data indicated that the accuracy and thermal properties of this circuit were marginal.

A second choice is a compensated log circuit as diagrammed below, which offers increased thermal stability with the use of a thermistor:[14]

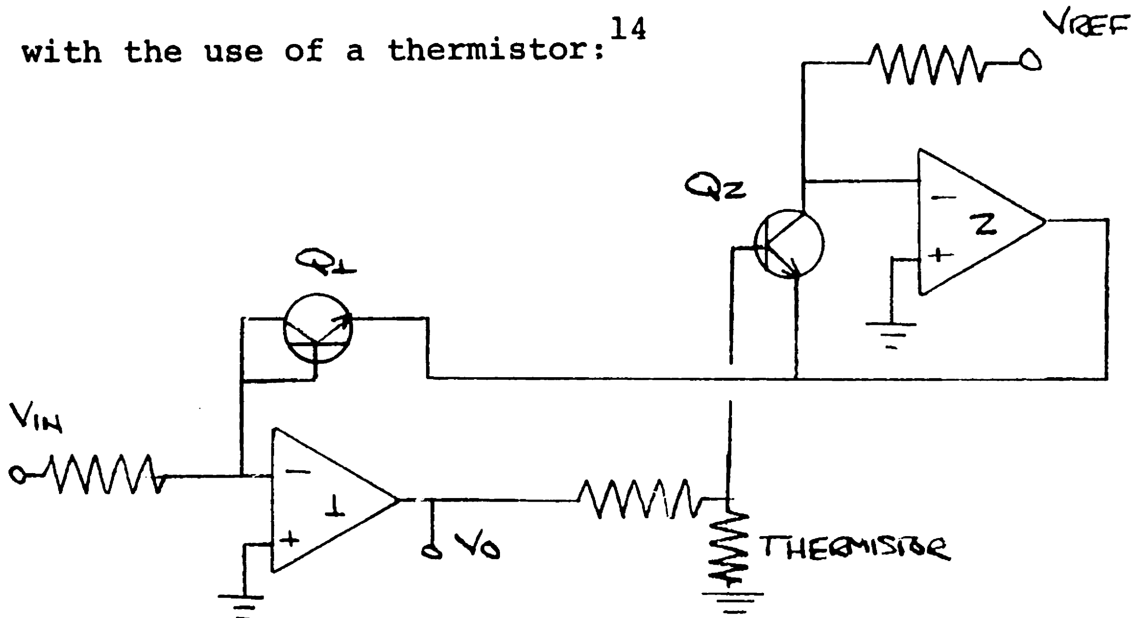

In the diagram, the collector of Q_2 is kept at virtual ground by the OP amp, and the collector current through Q_2 is equal to a constant reference current provided by V_{REF}. It can be shown that the output voltage is of the form $V_o = -\log_{10}\left(\frac{I_I}{I_R}\right)$ where the thermistor provides temperature compensation. One of the drawbacks to this scheme is that the number of components necessary to generate the log function has gone from 3 to at least 9, with proportional space and cost increases. This configuration was not evaluated.

The third and most expensive choice is to utilize a dedicated logarithmic device. The particular unit tested was a Texas Instrument log amplifier. This is a dual log generator on a single DIP package, at a cost of approximately $2.50. With appropriate circuit manipulation, the desired log/anti-log operations can be performed. The TI log amplifier was evaluated in depth. Results are documented in Appendix III. The log amplifier was the foundation of the simulator design. Other dedicated log/antilog modules exist which offer increased dynamic range, temperature stability, and accuracy, but alternative devices were an order of magnitude more costly than the TI log amplifier.

C. EXPONENTIATION - ALL CASES

In order to achieve either fixed or variable power exponentiation, the use of logarithms is basic. The signal flow for a fixed power exponent (power function generator or PFG) circuit is diagrammed below:

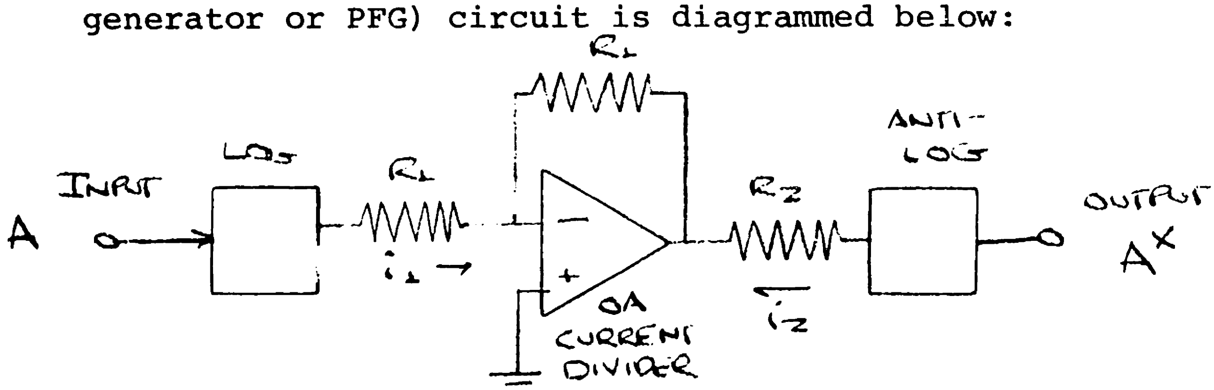

By a judicious selection of values for R_1 and R_2 current can be multiplied or divided using an operational amplifier in the ratio:

$$\frac{i_2}{i_1} \cong \frac{R_1}{R_2}$$

To be able to exponentiate to a variable power requires a cascaded log/antilog arrangement. The use of a segment of the state equations is made to demonstrate the concept. It is desired to generate the following:

$$XWC = K\left(1 - \left(\frac{PRC - 1}{BC}\right)\right)^{CC}$$

where K represents the scaling of several fixed parameters, and XWC, PRC, BC and CC are all problem variables. The circuit selected must process:

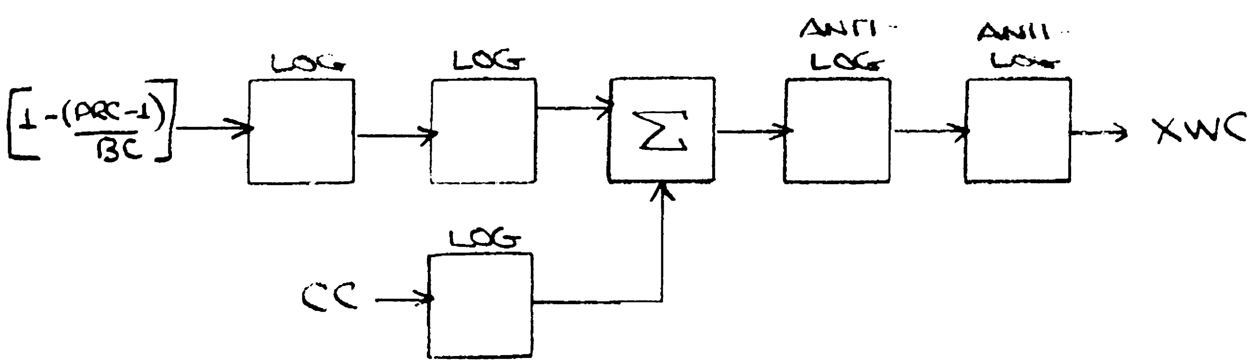

As a result of thermal instabilities, the interior section of the signal flow was replaced with a four-quadrant multiplier.

The multiplier essentially compresses the separate functions into a single chip. By circuit manipulation, a multiplier can also divide, square, and take square roots. A range of multiplier devices currently exist, with the price of the least expensive about $3.

Test data on the multiplier used in the simulator was collected in Appendix III. To allow as compact a circuit as possible, the multiplier was frequently utilized in its dividing and exponentiating modes. Complete device specifications are included in Appendix VI.

V. PRELIMINARY DESIGN

A. INTRODUCTION

The simulator design proceeded in a parallel fashion. In an iterative process, estimations were generated for the electronic layout, which allowed the cabinet and control panel to be sized and designed.

The simulator is configured to resemble a real-world engine control panel. Additional concepts for the peripheral design which were not incorporated were:

1. Proportional fuel control schemes with variable gains.
2. Torque-speed loads characteristic of pumps, propellers, generators, and other real world devices.
3. Cverspeed alarms and stall audio noise circuits.

B. ELECTRONICS

1. Logic Circuit

The logic processing of the electronic circuitry was broken down into 3 separate grid structures, which appear as design drawings in Appendix V. Use was made of bread-board panels to avoid the inflexibility of other techniques. Concurrent with testing various mathematical operations, the circuit design was modified to balance the competing parameters of simplicity, size, accuracy, and cost. The appropriate equation variables were normalized about their design point values, and then scaled to provide a circuit signal that was approximately 75% of the maximum rates input for the device. The steady state design point values for all variables were established by a DYSYS program and used for the normalization. Additional notes on the wiring techniques and breadboard layout are included in Appendix VI.

2. <u>DYSYS Simulation and Scaling</u>

A DYSYS simulation of the system equations was run as it appears in Appendix IV. Significant comments on the program are:

1. The conditional value of FC was changed to a fixed value of 3.0 to facilitate the circuit logic.
2. Markunas estimated a parabolic "pump-type" load torque, which appears as .0000977(3)**2.
3. The modeling parameter DT is called TT in the program to avoid confusion with the DYSYS time-step variables, DT.

The scaling procedure started with the following listings:

a. Constants

P_{o2}, P_{o5}	=	2041 LBF/FT^2
T_{o2}	=	539.7° R
γ	=	1.4
R	=	53.4 FT-LBF/LBM °R
C_p	=	.241 BTU/LBM-°R
h_{LHV}	=	16994 BTU/LBM

b. Machine Characteristics

$$I = 25 \text{ FT}^4$$

$$\left(\frac{N_G}{\sqrt{T_{o2}}}\right)_{DESIGN} = 309.8$$

$$\left(\frac{N_G}{\sqrt{T_{o4}}}\right)_{DESIGN} = 171.1$$

$$\left(\frac{\dot{m}_3\sqrt{T_{o2}}}{P_{o2}}\right)_{DESIGN} = 1.133$$

$$\left(\frac{\dot{m}_3\sqrt{T_{o4}}}{P_{o3}}\right)_{DESIGN} = 4096$$

c. <u>Input Variables at Design Point</u>

$\dot{m}_F$	=	1.1807 LBM/SEC
P_3	=	5028 FT-LBF

d. <u>State Variables at Design Point</u>

P_{S3}	=	102[illegible] LBF/IN^2
N_G	=	7200 RPM
T_{C4}	=	1731 R

The DYSYS simulation was run to verify Markunas's simulations. Use was made of the program to assist in adding voltage and current values to the circuit design, and to evaluate the effect of fixing the discontinuous constant, FC. FC was conditionally assigned the value of 2 or 4 in Markunas work. The steady state effect of assigning FC as 3 was investigated and adopted.

The DYSYS simulation was also run off - design to generate a test case for the logic circuit. The simulation was run at approximately 50% fuel flow and steady-state values were generated for all elements of the equations.

Some difficulty was encountered in determining the correct value for the lumped parameter fluid volume. The value which appeared to be consistent with Markunas' data was 144 ft^3. An approximation based on real world data gave 15 ft^3 as a more likely figure. Since the volume represents a time constant scaling for the fluid capacitance, it has no significance for the DYSYS steady state values. Changes in the volume assumed can be readily investigated in the simulator dynamic response.

The scaled voltage values and the system variables they represent are drawn on the 3 circuit plans in Appendix V.

C. PERIPHERALS

The main elements of the remaining design work included the chasis, power supply and distribution, instrumentation and control hardware, and breadboard architecture. The design drawings and sketches included in Appendix V illustrate the final peripheral design. The photograph below shows the internal layout of the simulator.

Appendix VI, specifications, contains additional data on the peripheral equipment, its wiring, and operating parameters.

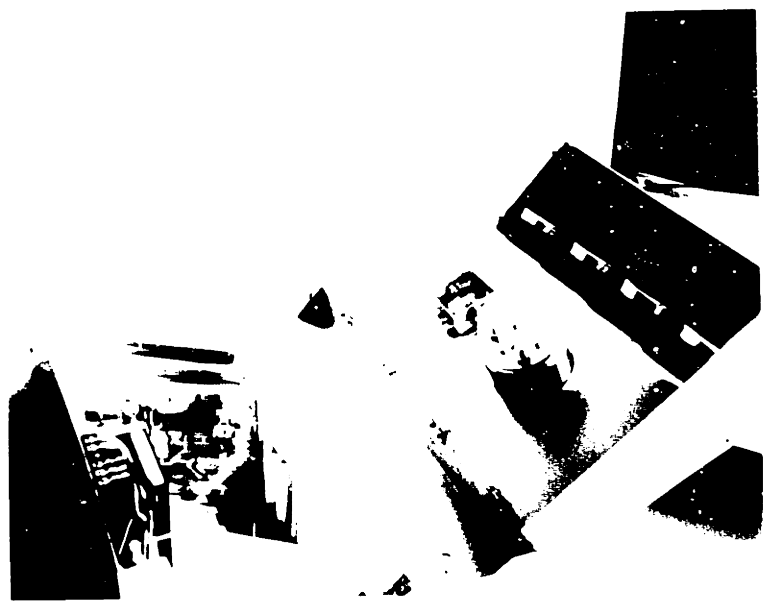

VI. IMPLEMENTATION AND CHECKOUT

A. PROCEDURE

To establish the characteristics of the various devices and to investigate the methodology of the design, 10 tests were conducted. The significant results are discussed here in the context of the design process. All test data is included in Appendix III.

B. LOG GENERATION

Tests 1 and 2 determined the voltage - current relations for the transdiode - connected OP amp, using both 2N2222 and 2N2904 transistors. It became apparent that the allowable voltage values of the log circuit were so narrow that only current variations could be used for the signal, over about a 1 1/2 decade range of values.

C. POWER EXPONENTIATION

Tests 3, 4, 5, and 6 were designed to varify the fixed power exponentiation circuitry. A workable configuration was wired in test 6, using a current - dividing resistive network.

Tests 7, 8, 9, and 10 were conducted to validate the variable - power exponentiation procedure. The inability of the transdiode - connected OP amp to provide a stable cascaded log circuit led to the investigation of a 4 quadrant multiplier in Test 8.

The Exar 2208 multiplier characteristics were investigated to generate hookup diagrams, trimming values, and allowable voltage values.

With Test 9, a simple log/multiplier/simple antilog circuit was wired and observed. Stability was significantly improved, but was still considered below the accuracy level desired.

In Test 10, a Texas Instrument 441 log amplifier was tested to determine its log/antilog characteristics. The log-amp was incorporated into the variable exponentiation circuit and the stability evaluated. The steady state accuracy of the log amplifier in the variable exponentiation circuit was somewhat better than the simple log configuration. Since the dedicated log amplifier offered better compensation characteristics than the simple log configuration, it was substituted at all points in the circuit design.

D. GENERAL CIRCUIT DESIGN

Concurrent with the test sequence, the overall circuit design was changing as new test data was generated. The more significant problems which caused iteration of the circuit are briefly discussed. One immediate limitation exists using the TI log amplifier module. Looking at "TL 441 Transfer Characteristics" included in Appendix III, the log amplifier only has a useable output range of 0 - 450 millivolts. This can be doubled by wiring an OP amp to the input side of the log amplifier to use the dual input capability of the device. Still, the output accuracy is limited, since various offsets for multipliers and OP amps can easily reach 10 millivolts.

As a general rule, it was decided to trin the circuit at a limited number of points, rather than dealing with the offsets required for each component.

It was intended in the final circuit design to operate all components at one dual-polarity supply voltage. This choice nominally would be ± 8 volts, the maximum rating of the most sensitive device, the TI log amp. Test 10 demonstrated that significant nonlinearities were introduced into the multiplier characteristics if the supply voltage were reduced. Three solutions were postulated:

1. Run the multipliers at ± 15 volts, and the OP and log amps at ± 8 volts.
2. Compensate the multiplier to have linear characteristics at ± 8 volts supply.
3. Replace the multiplier modules with log amplifiers to process the same function.

The first choice was selected in an effort to keep the circuit design as simple as possible, in as much as the single - voltage supply was more of a packaging consideration than an electronic one.

VII. CONCLUSIONS AND RECOMMENDATIONS

A. FEASIBILITY OF THE DESIGN

From the test data collected, a real time simulation can be conducted with the logic circuits wired as designed. The techniques developed for the implementation of non-linear differential equations should be applicable to a wide range of system models.

Markunas defined his engine in essentially non dimensional or pseudo-dimensionless groups. It was not possible to investigate the ability of the simulator to represent different geometric machines, however, it is felt that future work will verify the utility of the simulator and the nonlinear model.

B. DESIGN REFINEMENTS

The simulator as designed could be significantly enhanced with more general torque and fuel control schemes. If the simulator could demonstate sufficient generality in modeling the behavior of real world gas turbines, an autonomous "observer" circuit could be configured for a wide range of engines. This observer device, using the logic developed in the simulator, could be an extremely compact unit. It could provide improved control of fuel, speed, temperature, and pressure dynamics. Such a circuit could be incorporated in one or two monolithic LSI chips, to be externally trimmed for a particular engine or operating condition.

REFERENCES

1. A. L. Markunas, "Modeling, Simulation, and Control of Gas Turbines", MIT Thesis, M.S., 1972.

2. H. M. Paynter, "First Interim Technical Report - Computer Simulation of the Power Conversion System for Nike-X Power Plants, DA-49-129-ENG-542, Arthur D. Little, Inc.

3. J. H. Horlock, Axial Flow Compressors, Butterworths Scientific Publications, London, 1958.

4. J. H. Horlock, Axial Flow Turbines, Butterworths Scientific Publications, London, 1966.

5. D. G. Shepherd, Principles of Turbomachinery, MacMillan Co., New York, 1956.

6. D. R. Ahlbeck, "Simulating a Jet Gas Turbine with an Analog Computer", Simulation, September 1966.

7. J. F. Sellers and C. J. Daniele, "Dyngen - A Program for Calculating Steady-State and Transient Performance of Turbojet and Turbofan Engines", NASA TN D-7901, 1975.

8. J. R. Szuch and W. M. Burton,"Real Time Simulation of the TF-30-P-3 Turbofan Engine Using a Hybrid Computer", NASA TM x 3106, 1974.

9. J. R. Szuch and K. Seldner, "Real Time Simulation of F-100-PW 100 Turbofan Engine Using the Hybrid Computer", NASA TM x 3261, August 1975.

10. Nishio and Sugiyama, "Real Time Simulation of Jet Engines with Digital Computers", ASME Publication 74-GT-19.

11. F. D. Jordan, M. R. Hum, and A. N. Carras, "An Analog Computer Simulation of a Closed Brayton Cycle System", ASME Paper 69-GT-50.

12. B. D. MacIssac and H. I. H. Saravanamuttoo, "An Investigation into the Dynamic Performance of a Variable Pitch Turbofan Using a Hybrid Computer", ASME Paper 76-GT-31.

13. B. D. MacIssac and H. I. H. Saravanamuttoo, "A Comparison of Analog, Digital, and Hybrid Computing Technique: for Simulation of Gas Turbine Performance", ASME Paper No. 74-GT-127.

14. J. K. Roberge, Operational Amplifiers: Theory and Practice, Wiley and Sons, New York, 1975.

15. W. C. Jung, IC OP-AMP Cookbook, H. W. Sams and Co., Indianapolis, 1977.

16. J. Carr, OP-AMP Circuit Design and Application, Tab Books, Blue Ridge Summit, PA, 1976.

17. D. H. Sheingold, NonLinear Circuits Handbook, Analog Devices, Norwood, MA, 1974.

18. K. Tracton, Integrated Circuits Guidebook, Tab Books, Blue Ridge Summit, PA, 1975.

19. RCA Transistor Thyristor and Diode Manual, Harrison, NJ, 1969.

20. The Linear Control Circuits Data Book for Engineers, Texas Instruments, Dallas, 1975.

APPENDIX I

MACHINE CHARACTERISTICS

MACHINE CHARACTERISTICS

FROM MARKUNAS[1]

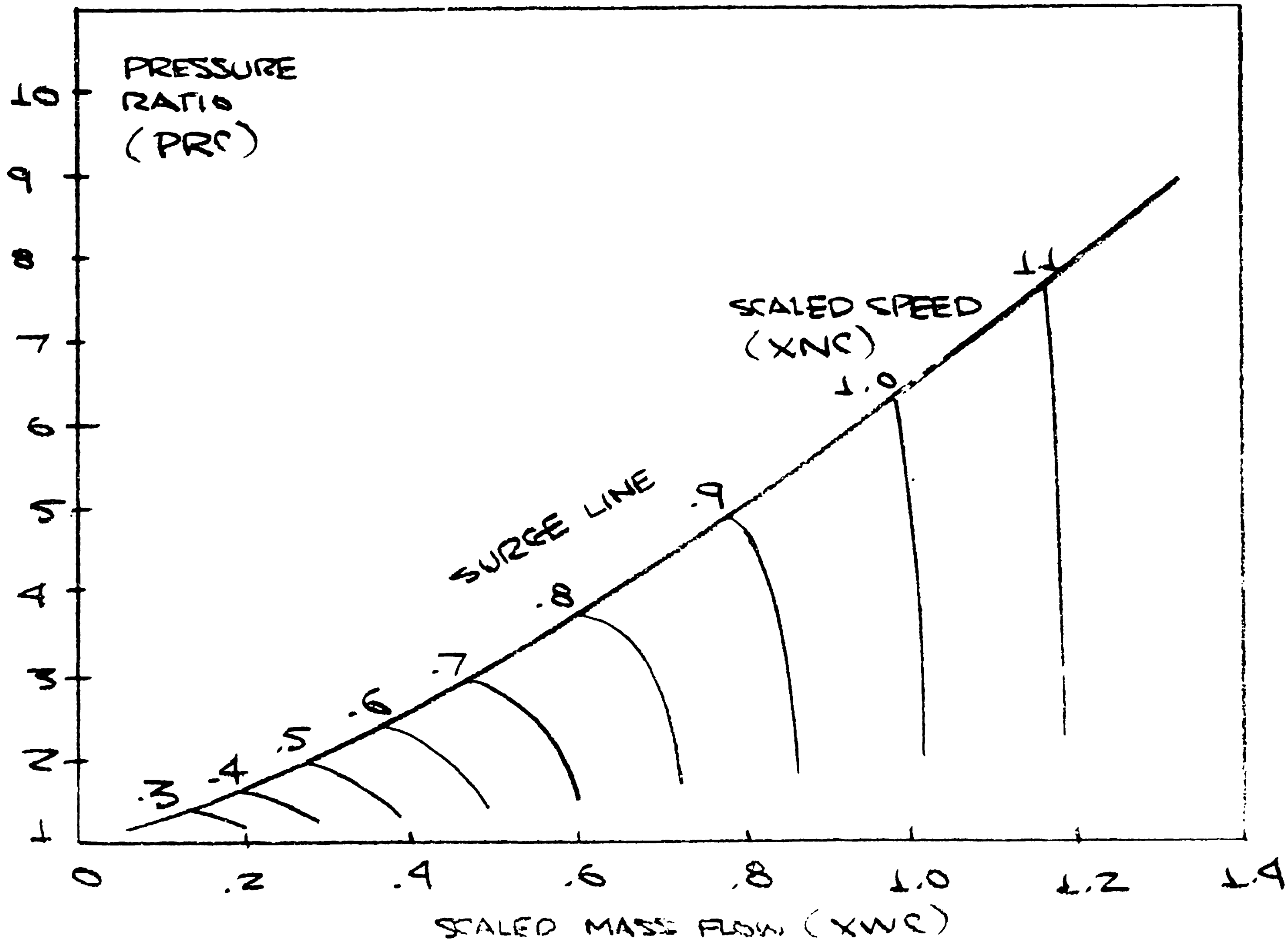

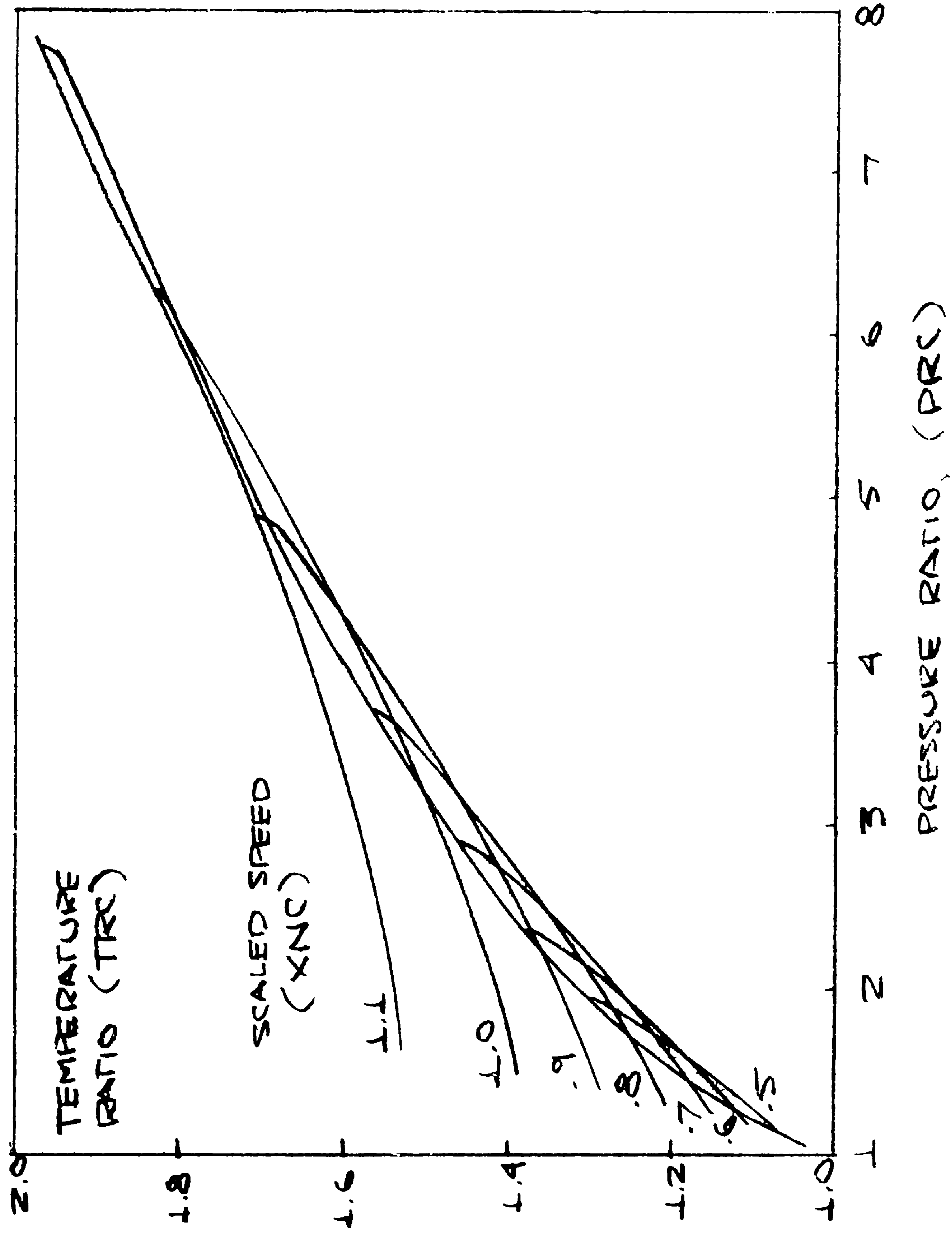
TEMPERATURE RATIO (TRC)
SCALED SPEED (XNC)
PRESSURE RATIO (PRC)
1
2
3
4
5
6
7
8
1.0
1.2
1.4
1.6
1.8
2.0
1.1
1.0
.9
.8
.7
.6
.5

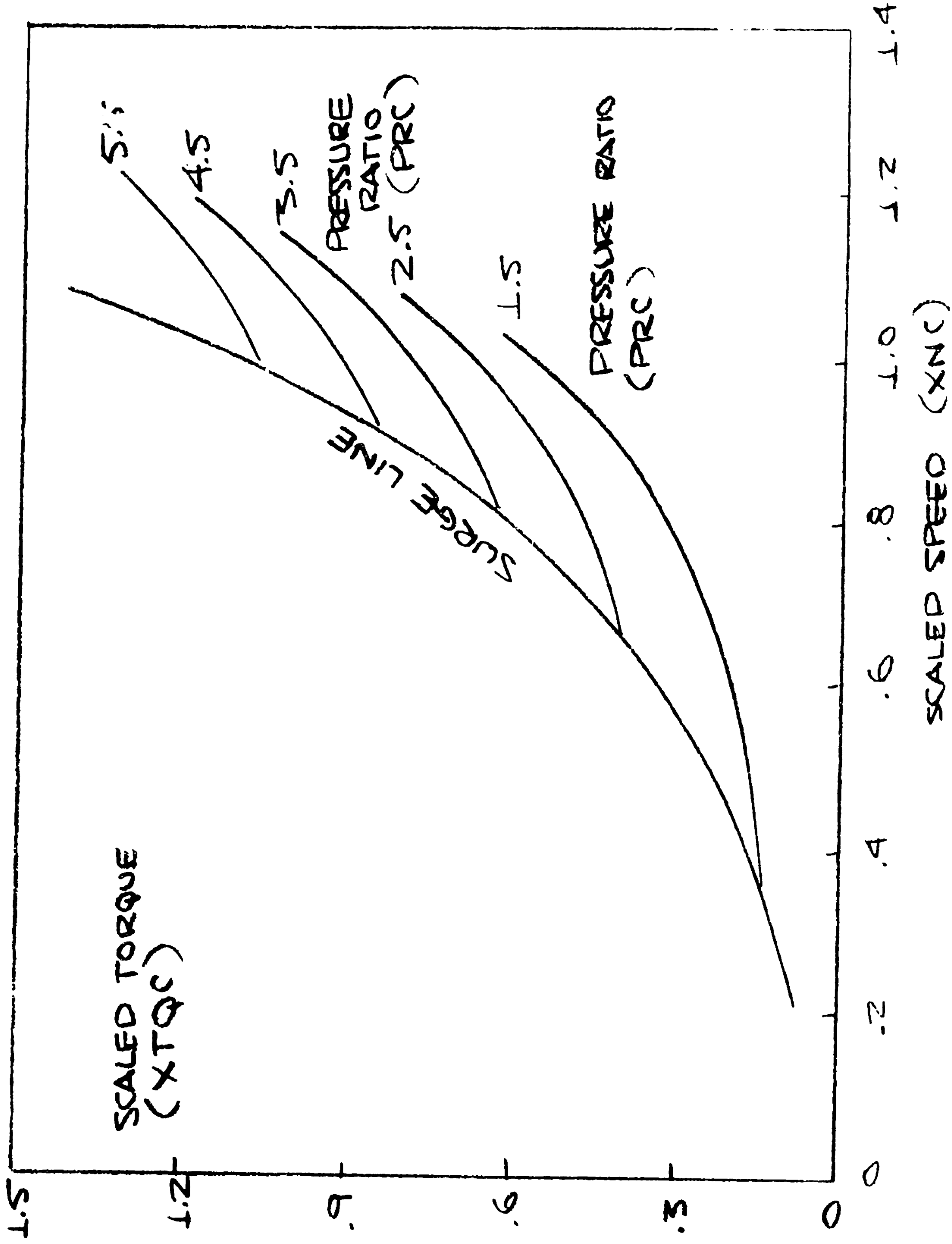

SCALED TORQUE (XTQC)
SCALED SPEED (XNC)
SURGE LINE
PRESSURE RATIO (PRC)
PRESSURE RATIO (PRC)
5.5
4.5
3.5
2.5
1.5
0
.3
.6
.9
1.2
1.5
.2
.4
.6
.8
1.0
1.2
1.4

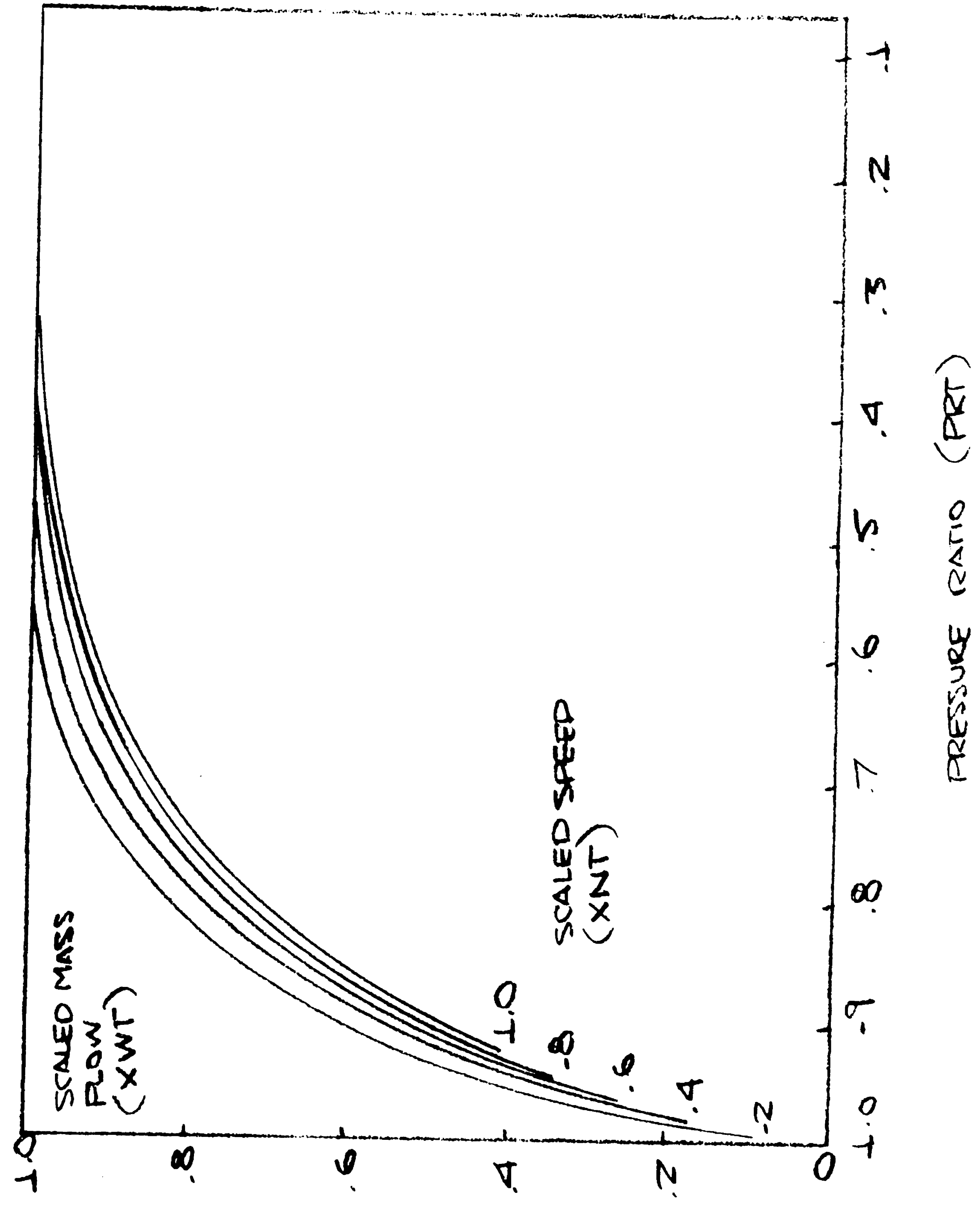
SCALED MASS FLOW (XWT)
SCALED SPEED (XNT)
PRESSURE RATIO (PRT)
1.0
.8
.6
.4
.2
0
.1
.2
.3
.4
.5
.6
.7
.8
.9
1.0

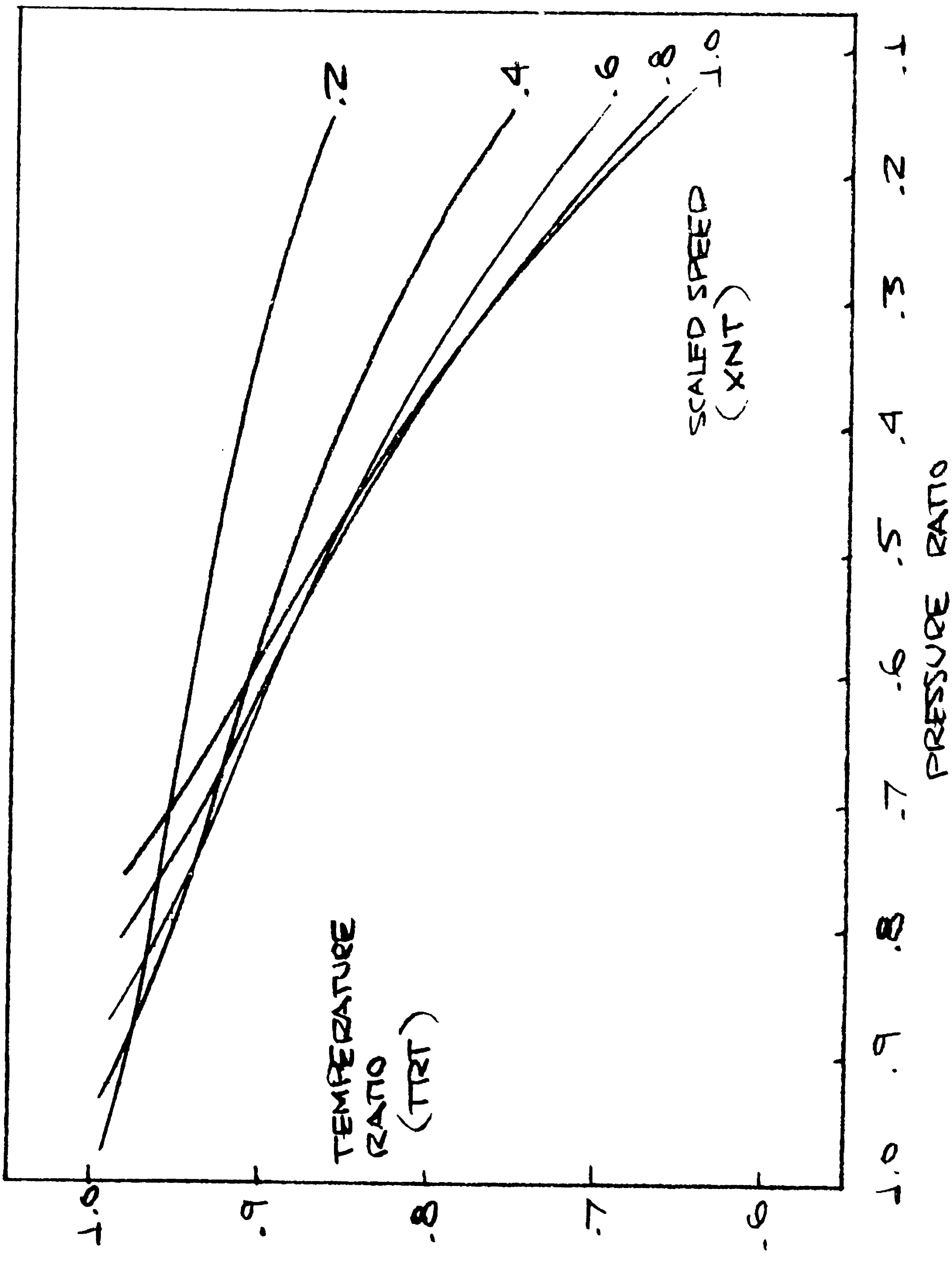
TEMPERATURE
RATIO
(TRT)
SCALED SPEED
(XNT)
PRESSURE RATIO
.2
.4
.6
.8
1.0
.1 .2 .3 .4 .5 .6 .7 .8 .9 1.0
1.0 .9 .8 .7 .6

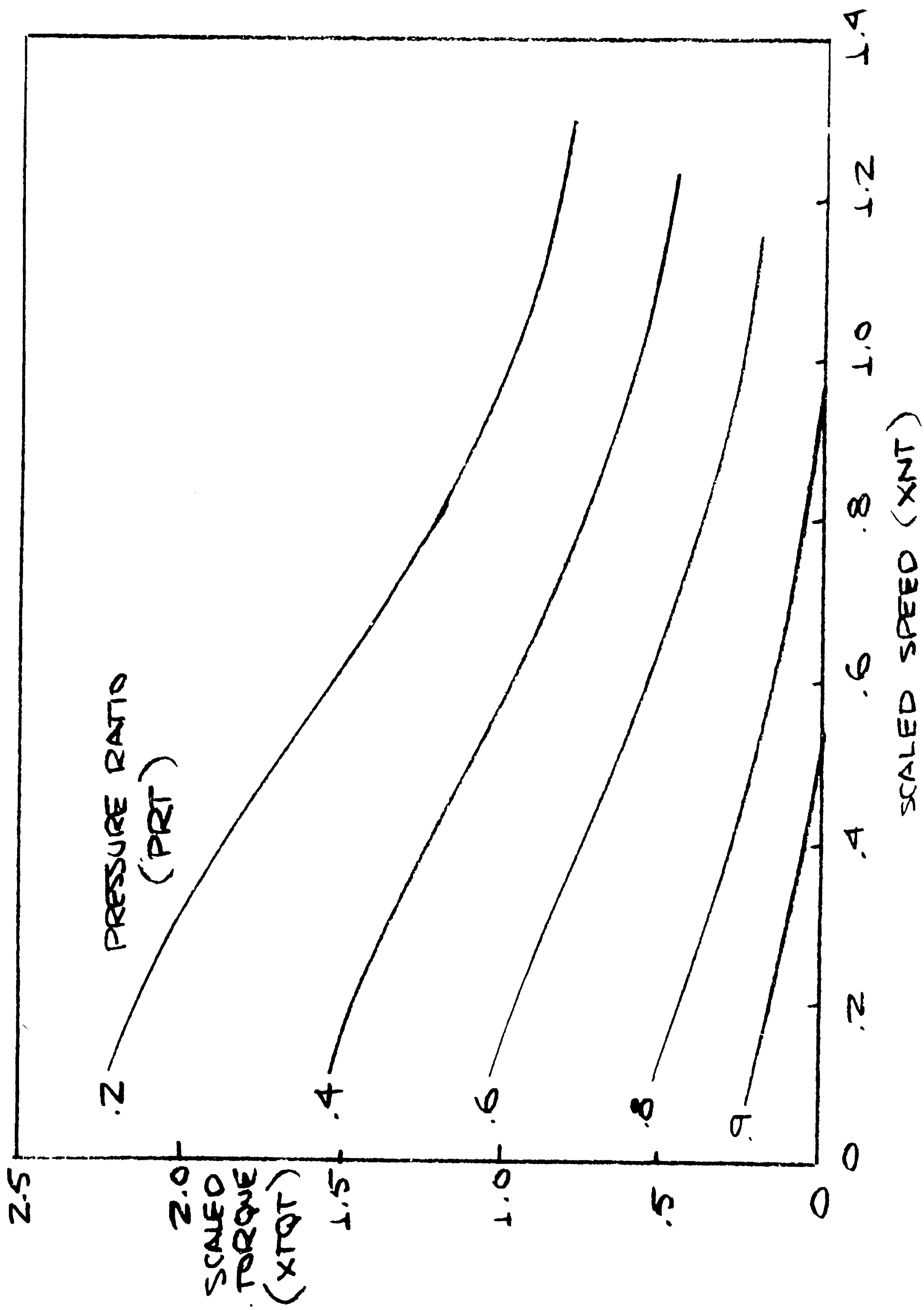
PRESSURE RATIO
(PRT)
.2
.4
.6
.8
.9
SCALED SPEED (XNT)
0
.2
.4
.6
.8
1.0
1.2
1.4
SCALED TORQUE (XTQT)
0
.5
1.0
1.5
2.0
2.5

APPENDIX II

STATE EQUATIONS

STATE EQUATIONS

I.

$$\dot{P}_{03} = \left(\frac{\overline{nRT_{04}}}{VOL}\right)\left[\dot{m}_3 - \dot{m}_4\right]$$

$$\dot{P}_{03} = \left(\frac{\overline{nRT_{04}}}{VOL}\right)\left[(XMC)(AC)(XWC) - (XMT)(AT)(XWT)\right.$$

II.

$$\dot{T}_{04} = \left(\frac{(n-1)\gamma R T_{04}}{n\, P_{03} Vol}\right)\left[\dot{m}_3 T_{03} + \dot{m}_F\left(\frac{h_{LHV}}{c_p}\right) - \dot{m}_4 T_{04}\right]$$

$$\dot{T}_{04} = \left(\left(\frac{n-1}{n}\right)\frac{\gamma R T_{04}}{P_{03} Vol}\right)\left[\left[(XMC)(AC)\left(1-\left(\frac{PRC-1}{BC}\right)\right)^{CC}\right]\left[T_{02} + T_{02}\left(\frac{(PRC)^{(GEC)}-1}{EFFC}\right)\right] + \dot{m}_F\left(\frac{h_{LHV}}{c_p}\right) - T_{04}(XMT)(AT)(XWT)\right]$$

WHERE

$$XMC = \frac{P_{02}}{\sqrt{T_{02}}}\left(\frac{\dot{m}_3\sqrt{T_{02}}}{P_{02}}\right)_{DESIGN}$$

$$XMT = \frac{P_{03}}{\sqrt{T_{04}}}\left(\frac{\dot{m}_4\sqrt{T_{04}}}{P_{03}}\right)_{DESIGN}$$

III.

$$\dot{N}_G = \frac{30}{\pi I}\left[T_2 - T_1 - T_3\right]$$

$$\dot{N}_G = \frac{30}{\pi I}\left[\frac{30 C_P}{\pi}\left[\frac{T_{04}}{N_G}\right](XMT)(AT)\left(1 - PRT^{BT}\right)^{CT}\left(2 - \left(1 - \left(1 - \sqrt{\frac{1 - .8(XNT)^{1.25}}{1 - PRT}}\right)^{2}\right)\right)\left[\left(1 - (PRT)^{GET}\right] - (XMC)(AC)(XWC)(T_{02})\left(\frac{TRC - 1}{N_G}\right)\right] - T_3\right]$$

APPENDIX III

Test Data

A. TEST 1 AND 2

From reference data,[19] the transdiode voltage current characteristics was estimated for various values of saturation current. The log circuits diagrammed subsequently for the 2N2222 and 2N2904 transistors demonstrated low base-emitter saturation currents, thus making the exponential characteristic curve more abrupt.

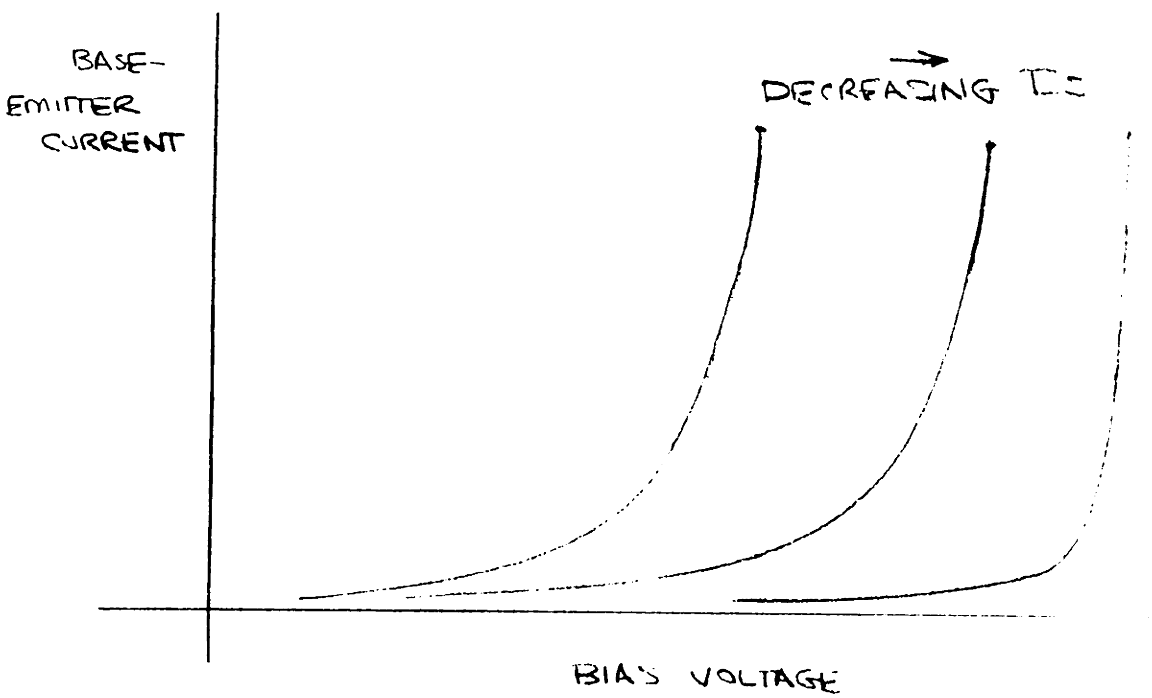

Test Data

$$I = I_s e^{(E_o/26Mv)}$$

E_o(Mv)	I (MA)	Estimated IS (PA)
470	.004	5.04×10^{-11}
548	.015	1.05×10^{-11}
581	.045	8.87×10^{-12}
609	.121	8.13×10^{-12}
616	.178	9.14×10^{-12}

Test Circuit

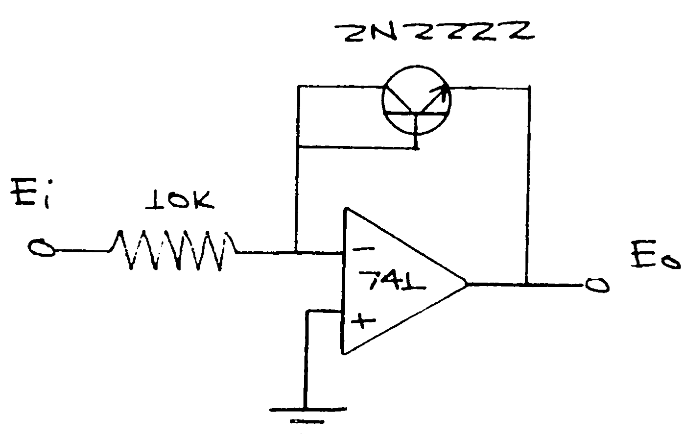

TEST 2

CIRCUIT DIAGRAMS AND DATA

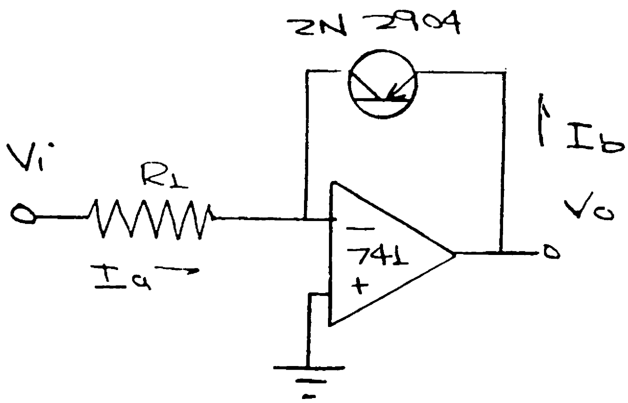

R1 = 10K

Vi (VOLTS)	Ia (mA)	Vo (mV)	Ib (mA)
-4.82	.161	580	[illegible]
-4.32		[illegible]	[illegible]
-3.95	.133	[illegible]	.138
-2.12	.070	565	[illegible]
-1.71	.057	559	.060

R1 SWITCHED TO 30K

Vi (VOLTS)	Vo (mV)
-.003	384
-.011	423
-.021	445
-.044	465
-.071	476
-.106	487
-.142	502
-.251	509
-.354	511
-.430	523

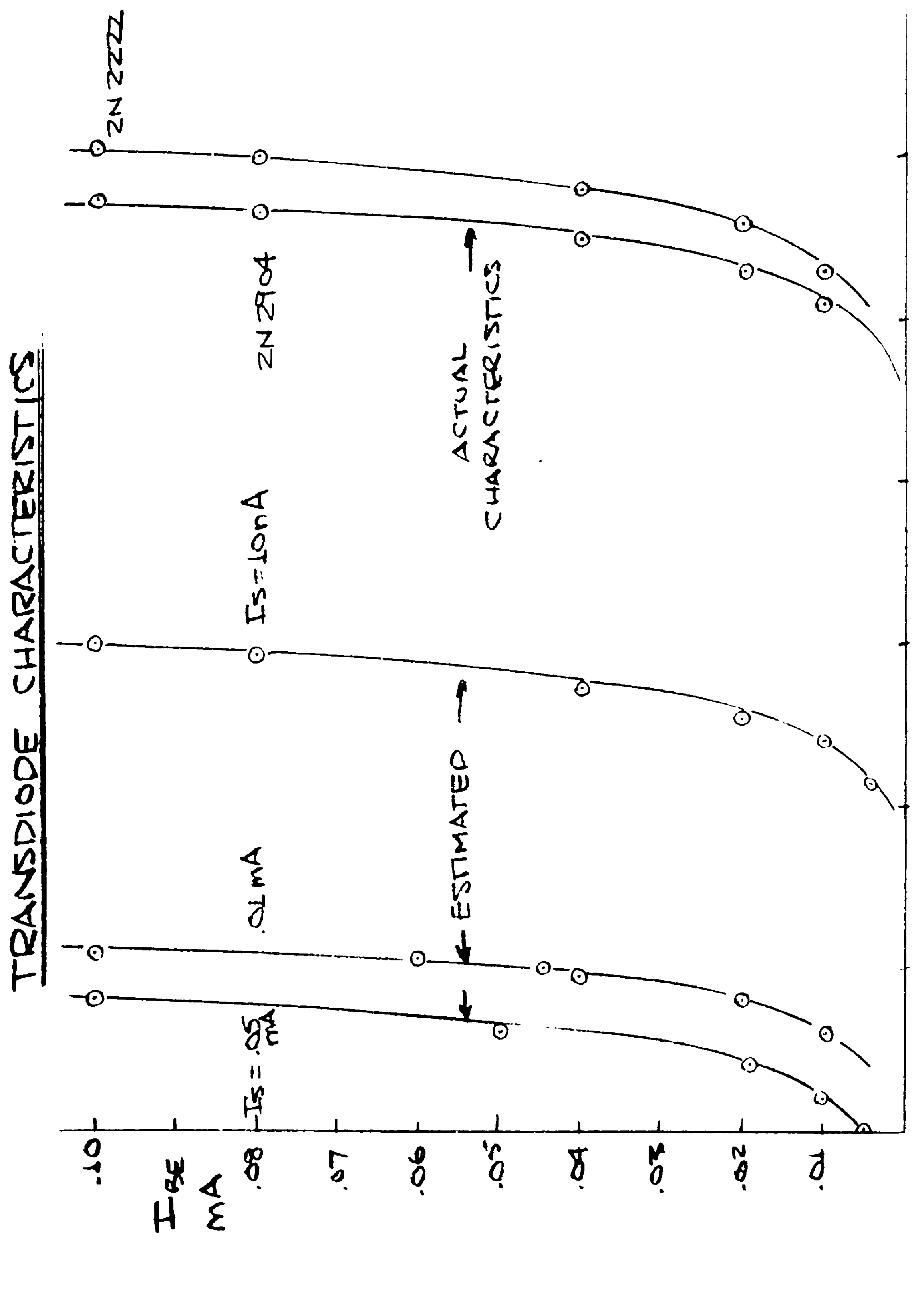
TRANSDIODE CHARACTERISTICS
2N 2222
2N 2904
ACTUAL CHARACTERISTICS
ESTIMATED
Is = 10nA
.1mA
Is = .05 mA
BIAS VOLTAGE MILLIVOLTS
100
200
300
400
500
600
I_BE
mA
.10
.08
.07
.06
.05
.04
.03
.02
.01

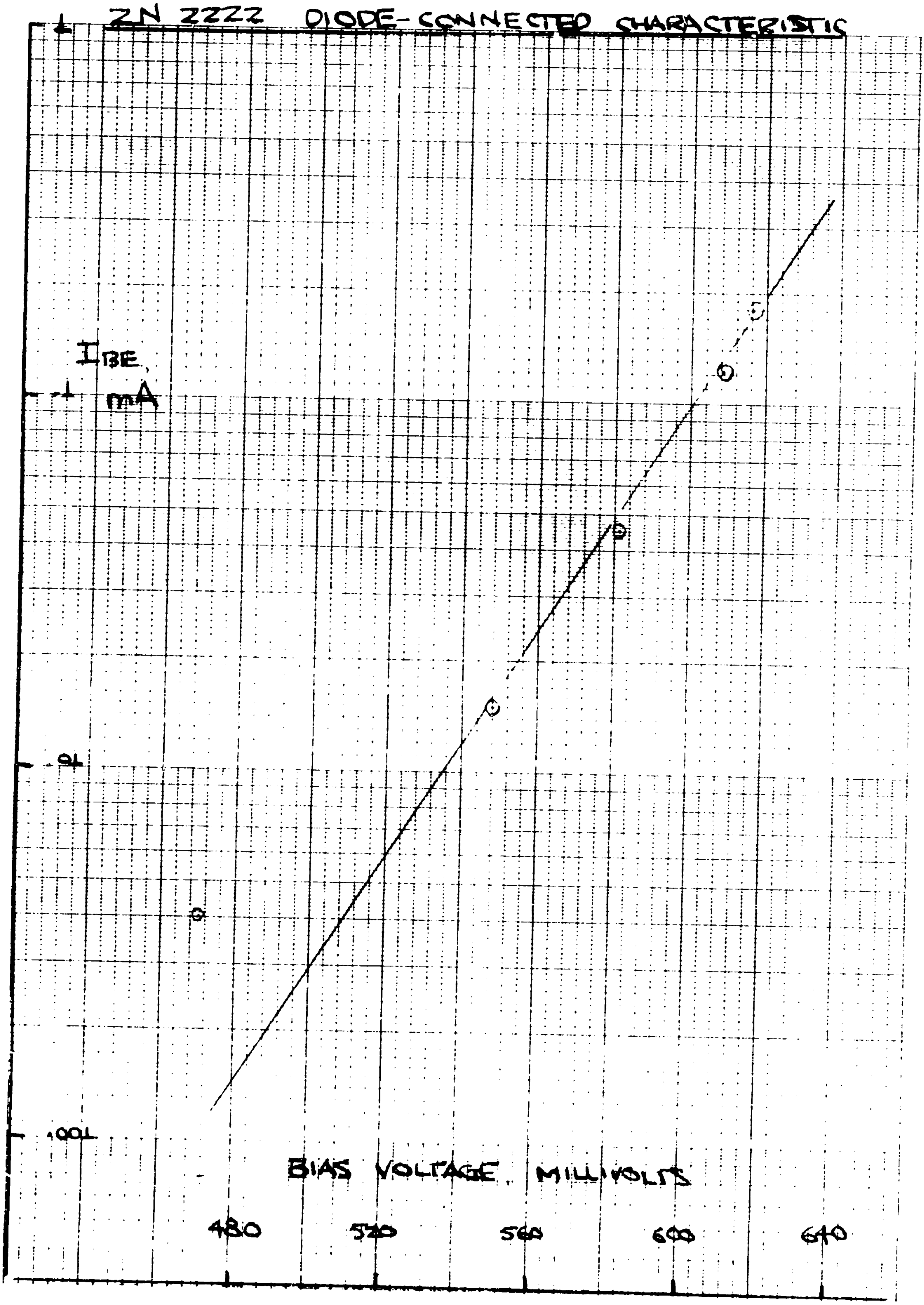
2N 2222 DIODE-CONNECTED CHARACTERISTIC
I_{BE} mA
1
.01
.001
BIAS VOLTAGE MILLIVOLTS
480
520
560
600
640

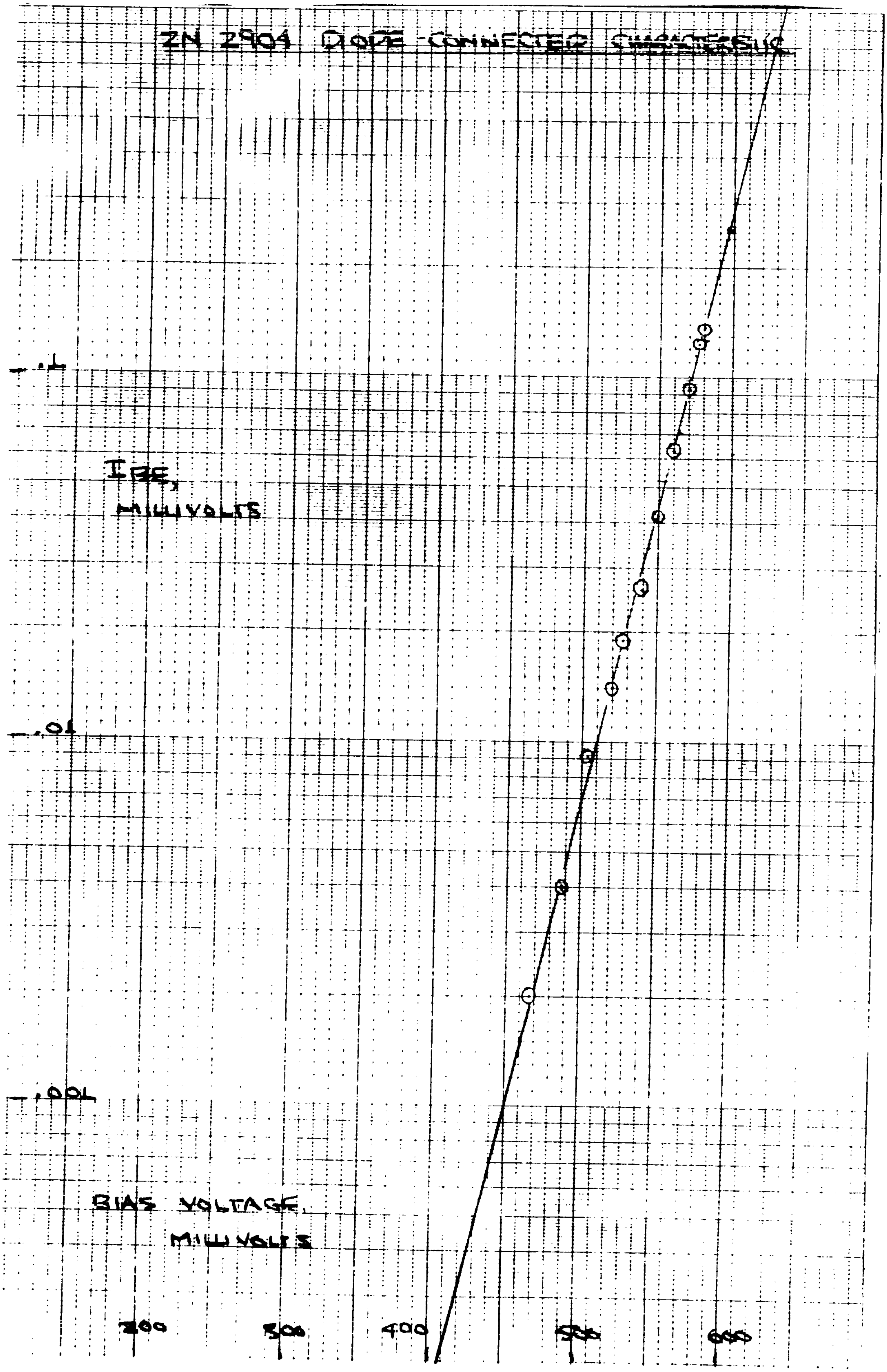
2N 2904 DIODE CONNECTED
IBE,
MILLIVOLTS
.1
.01
.001
BIAS VOLTAGE,
MILLIVOLTS
300
400
500
600

B. TESTS 3 - 6

The fixed exponentiation of a variable was evaluated in Tests 3 - 6. Tests 3, 4, and 5 were failures as the essential concept of current division to achieve the exponentiation was not understood. Test 6 demonstrates the use of a resistive network which accomplished the current manipulation. It is now apparent that as a result of the characteristics of the simple log configuration, current division can be easily accomplished by assigning the appropriate resistor value to the antilog input. This is diagrammed:

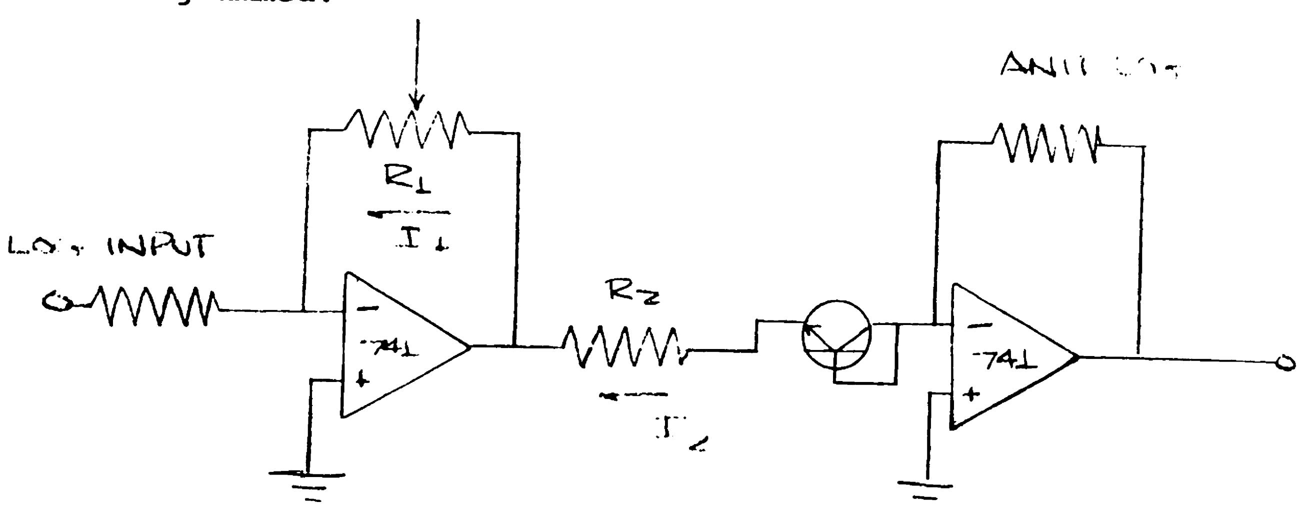

$$\frac{I_2}{I_1} = \frac{R_1}{R_2}$$

TEST 3

CIRCUIT DIAGRAMS AND DATA

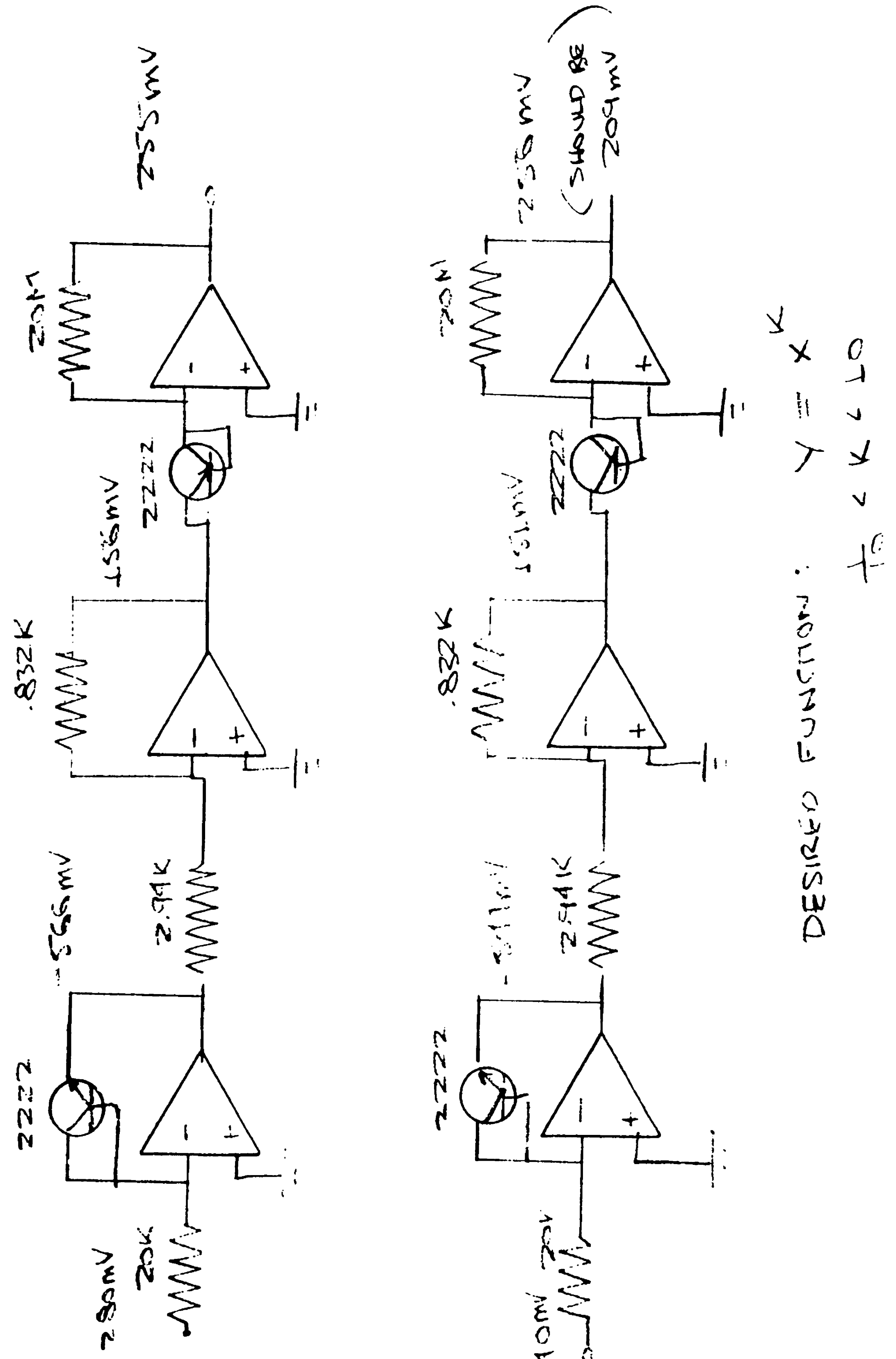

TEST 4

CIRCUIT DIAGRAMS AND DATA

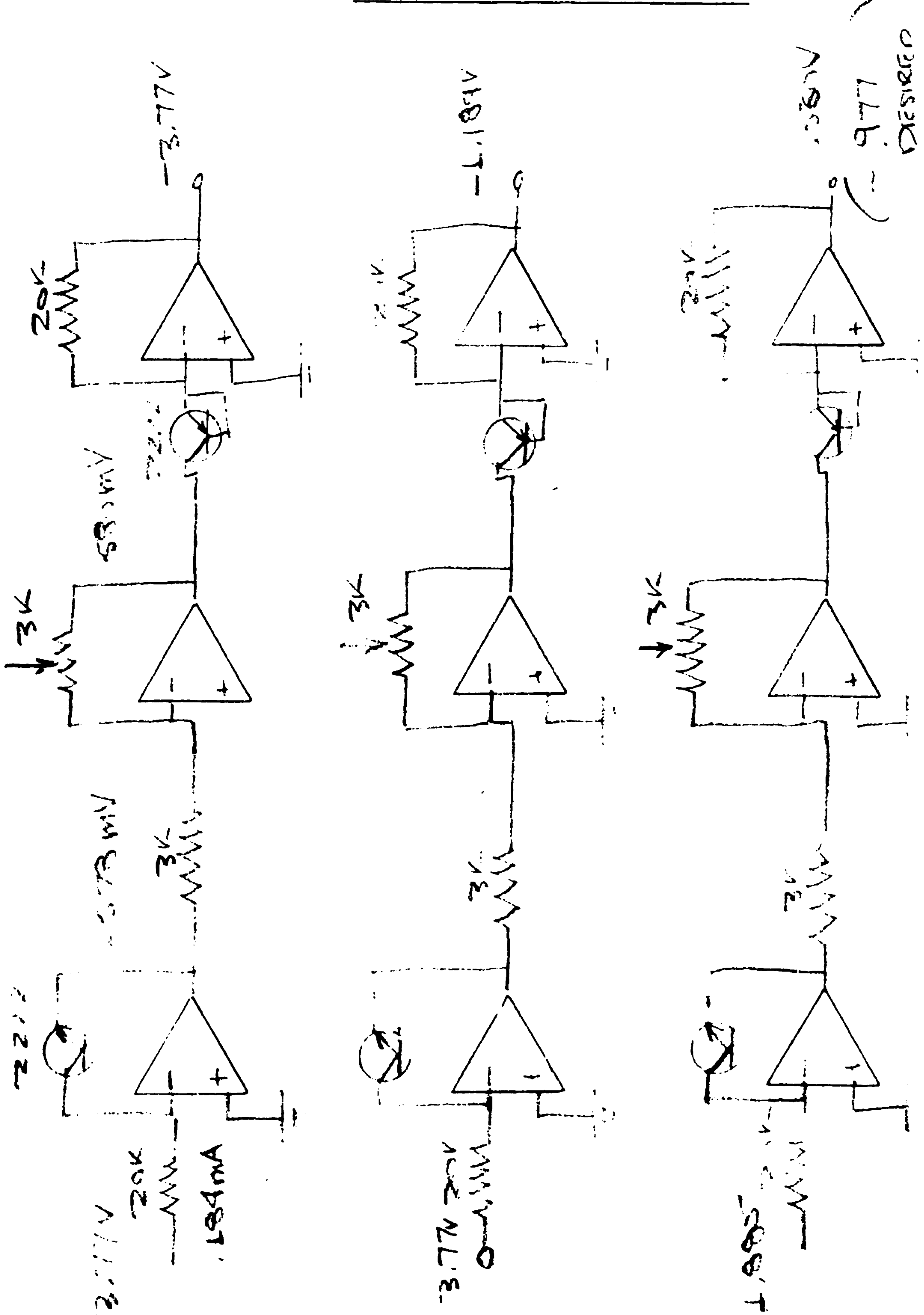

TEST 5

CIRCUIT DIAGRAMS AND DATA

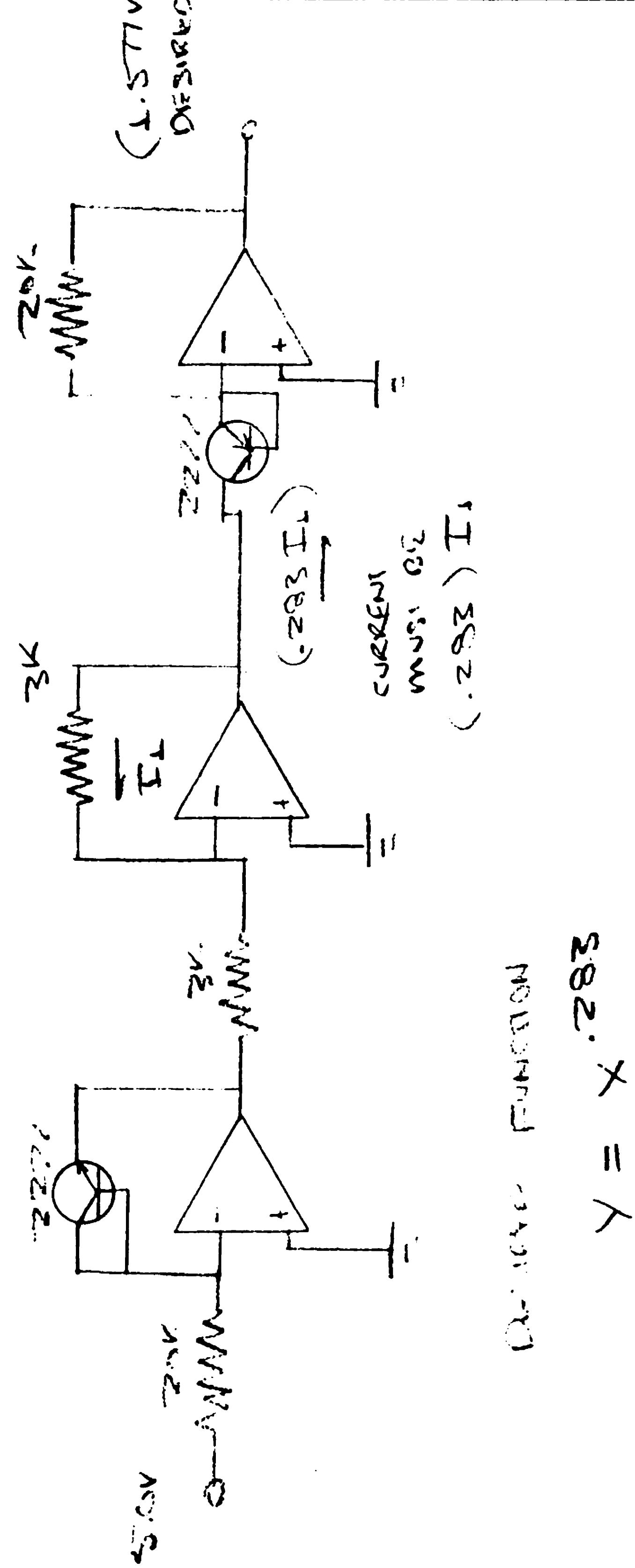

TEST 6

CIRCUIT DIAGRAMS AND DATA

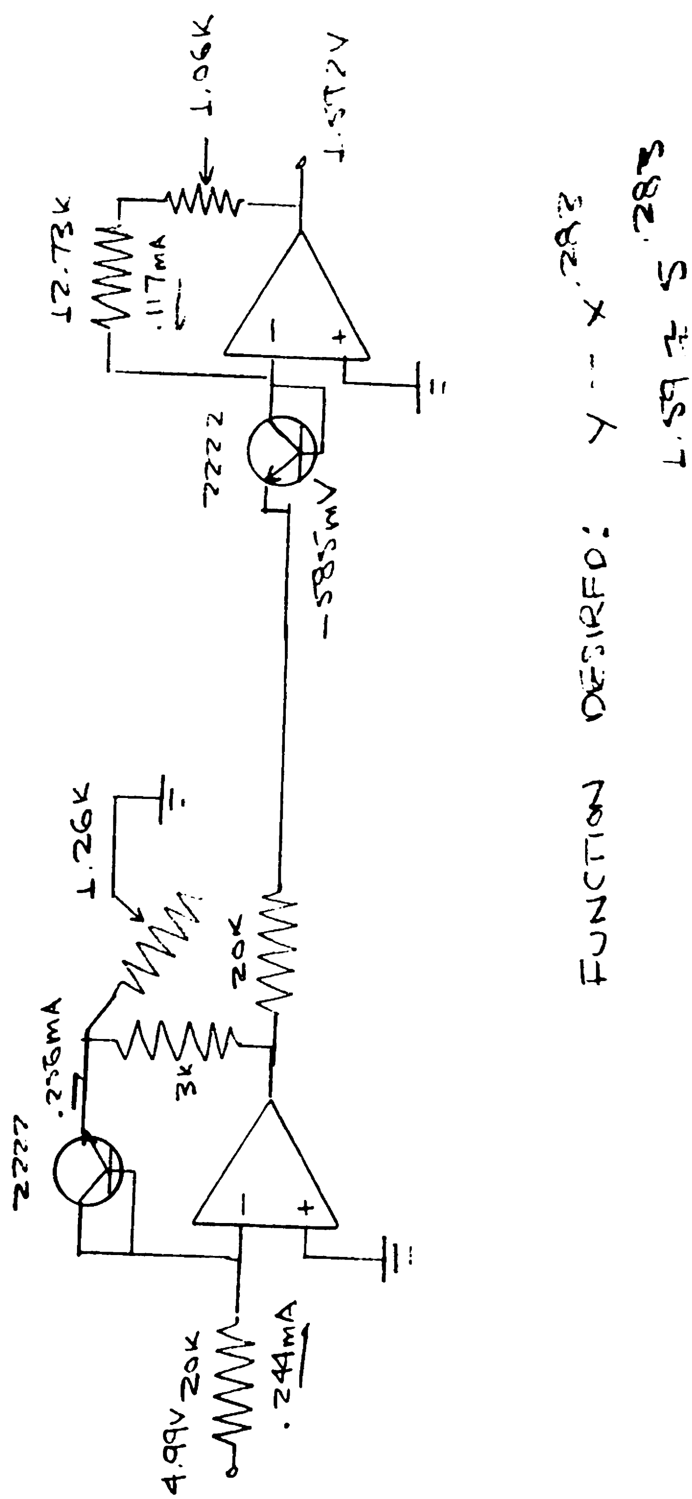

C. TEST 7

It is desired to validate the circuit segment for the operation

$$\left(1 - \left(\frac{PRC - 1}{BC}\right)\right)^{CC}$$

The operational sequence is as follows:

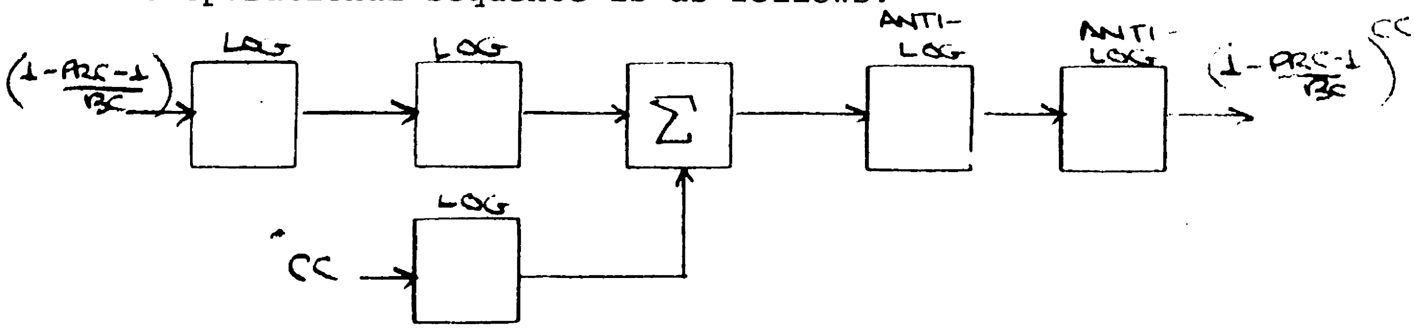

The circuit described in the test data was set up to evaluate the feasibility of the operation.

The desired operating characteristic of the cascaded logger - antilogger is picutred as follows:

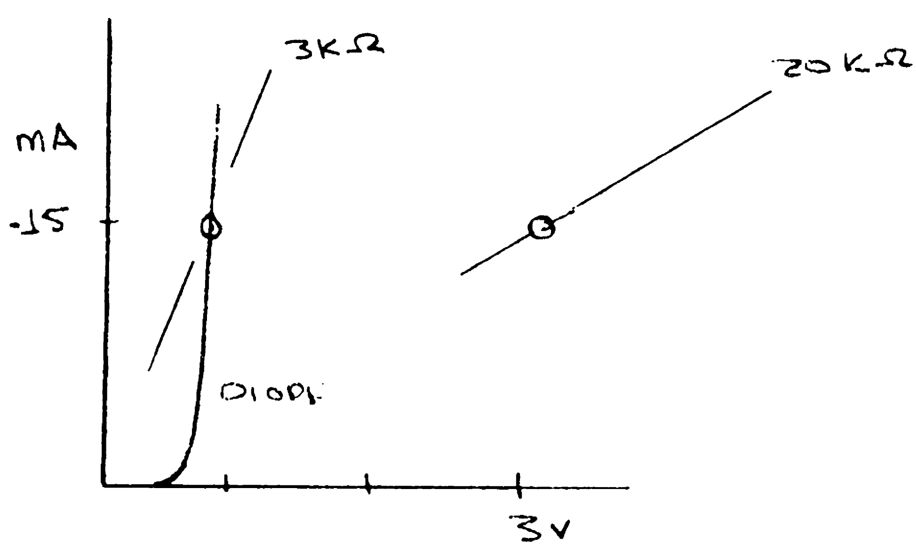

The first log geneator establishes a voltage - current relation based on the diode and 20K resistor. Consider the second log generator to be superimposed in the first with a 3K resistor and a second diode.

The cascaded antilog - configured amplifiers displayed gross thermal sensitivity. The simple OP amp - transdiode configuration is unsuitable for this cascaded operation without additional temerature compensation.

TEST 7

CIRCUIT DIAGRAM

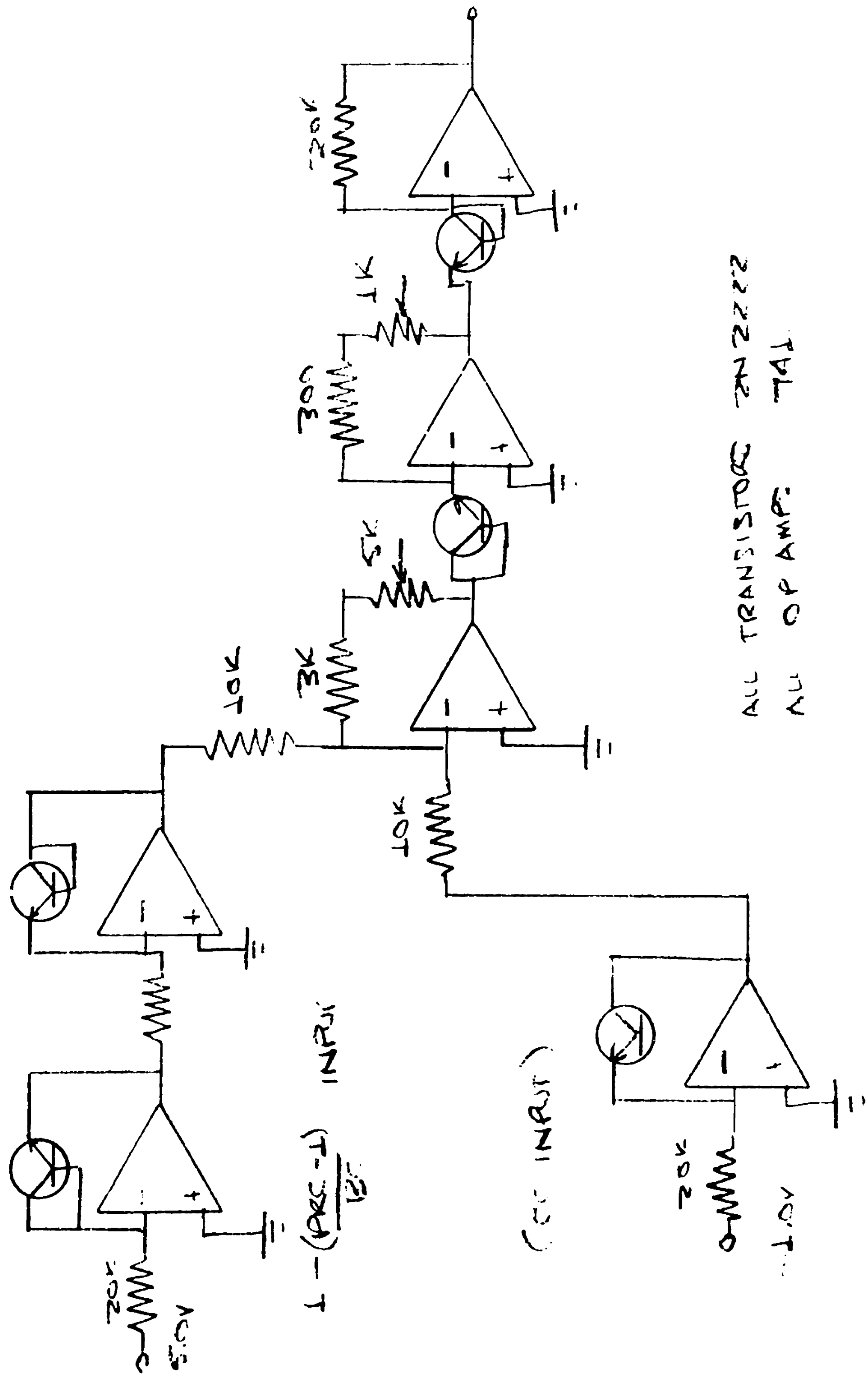

D. TEST 8

i. Purpose

Test 8 was conducted to verify the variable exponent part of the analog circuitry, using the four quadrant multiplier.

The equation of interest is written below:

$$\dot{M}_3 = \left(1 - \left(\frac{PRC - 1}{BC}\right)\right)^{CC}$$

LOOKING AT THE LOGIC FLOW:

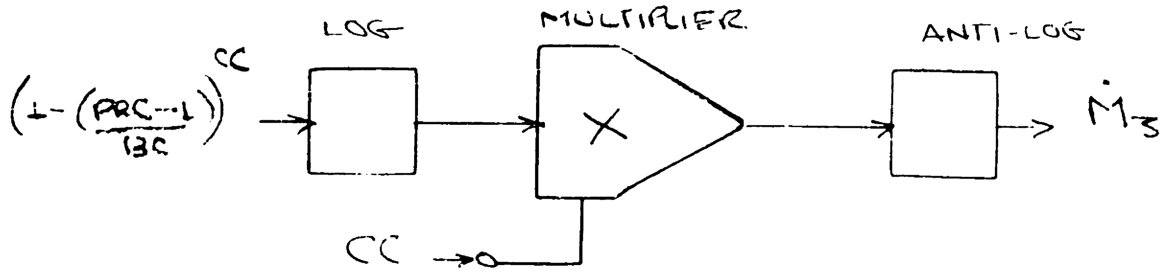

ii. Methodology

The functional method used to exponentiate to a variable power was to regulate the multiplier output current in the ratio called for by the exponentiation. For example:

IF CC = .018

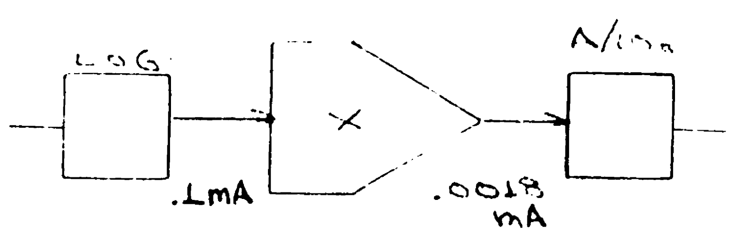

For multiplier scaling the integral buffer OP amp in the 2208 was used for the current division with a resistive bridge as follows,

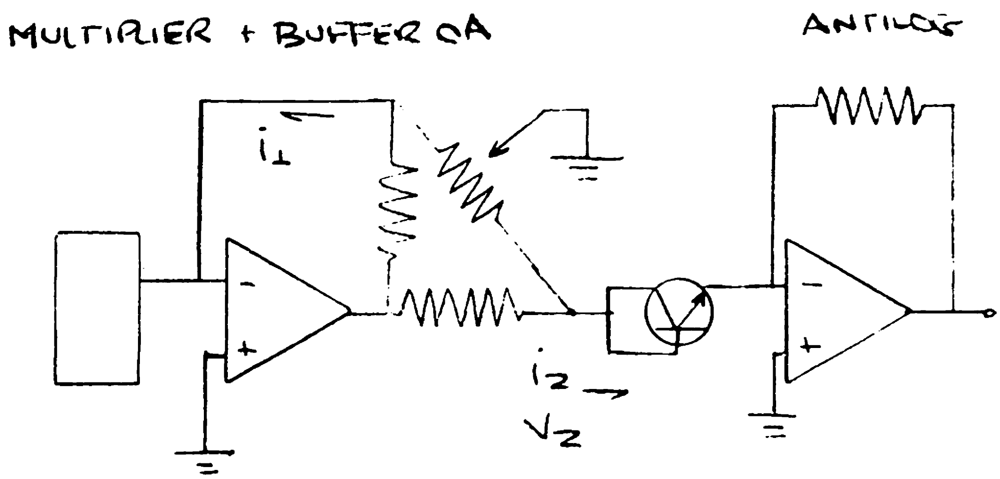

such that $i_1 = i_2$ and the output voltage of the multiplier is thus controlling the current input to the antilog amplifier transdiode.

The multiplier output is nominally:

$$V_z = \frac{V_x V_y}{10}$$

TO OBTAIN $V_z \leq 600$ mV, RESISTANCE VALUES MUST BE SELECTED TO GET THE DESIRED RANGE OF ANTILOG INPUTS.

It was determined that a resistive bridge must be used for the multiplier input from logging OA, sketched as follows:

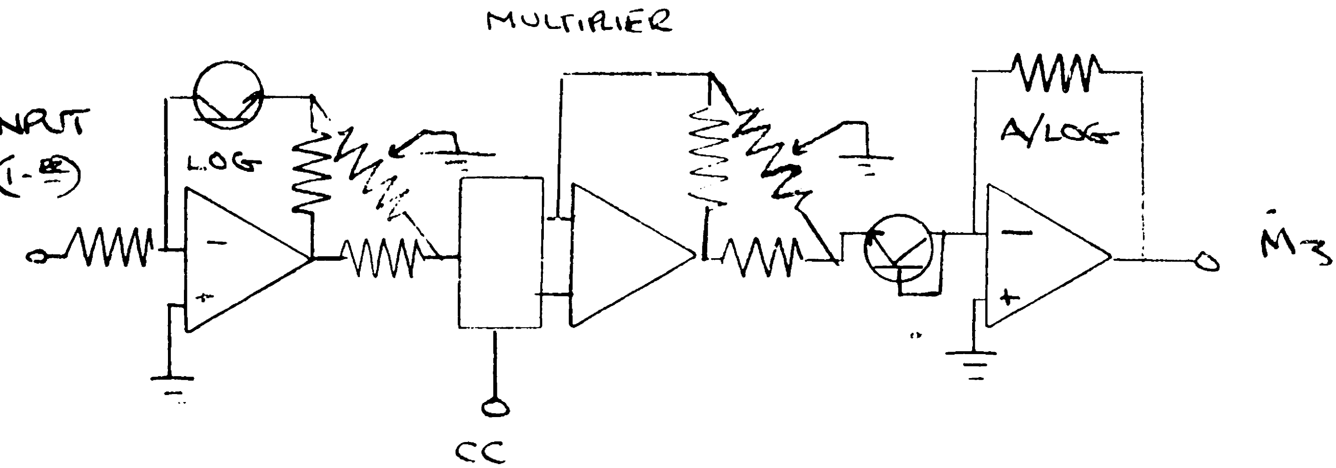

so by modulation of CC input, the desired current ratios across multiplier can be achieved.

iii. Data

A 5 minute observation of the steady state output voltage was made to investigate the circuit thermal stability.

10 Second Samples — -Volts x 10

.630	.650	.639
.635	.643	.634
.625	.671	.634
.667	.649	.640
.644	.651	.642
.635	.651	.629
.630	.659	.631
.624	.641	.626
.661	.652	

26 Samples

MEAN = .642

STD DEVIATION = .0137

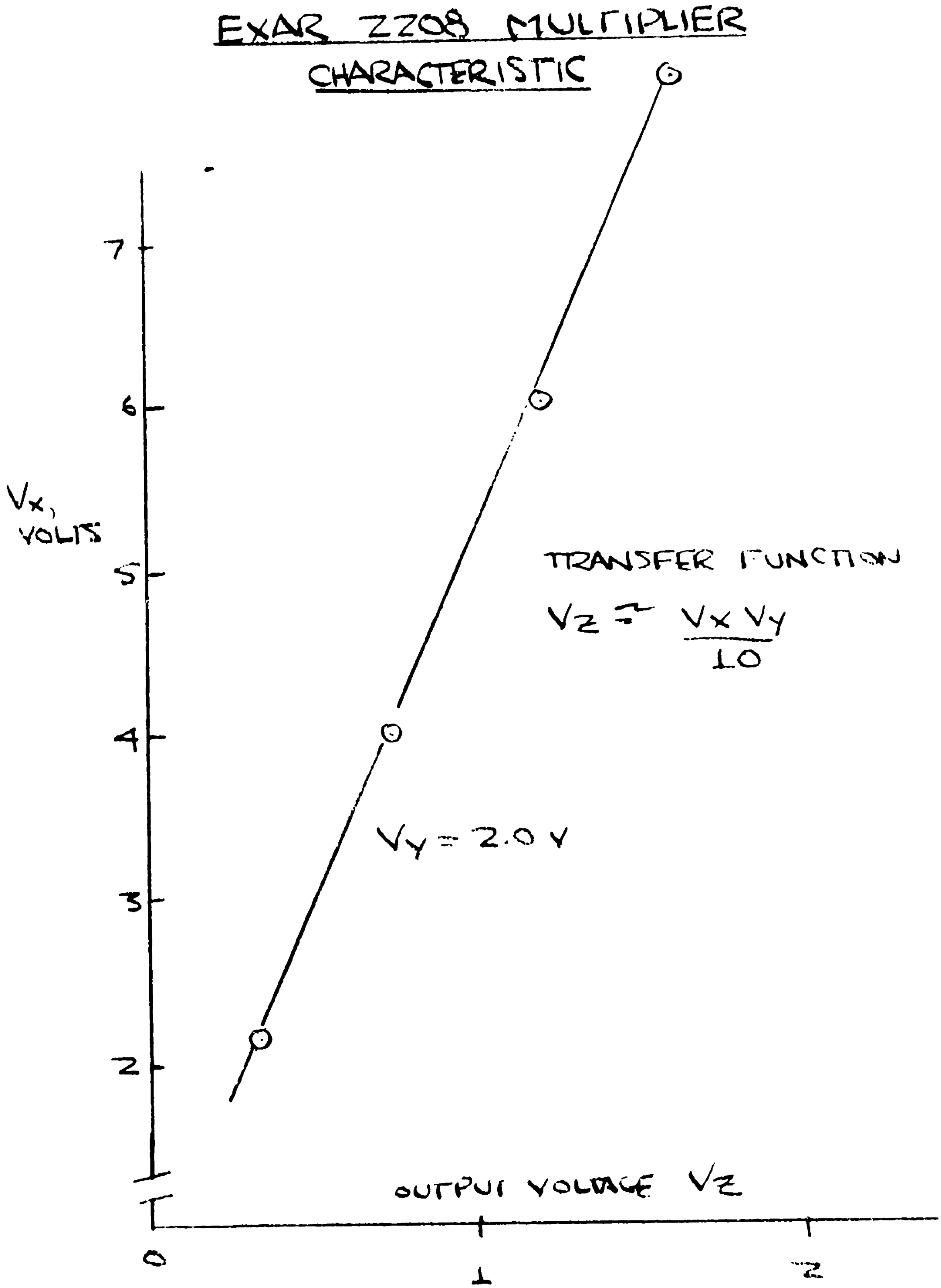
EXAR 2208 MULTIPLIER
CHARACTERISTIC
Vx, VOLTS
7
6
5
4
3
2
TRANSFER FUNCTION
$V_Z = \frac{V_X V_Y}{10}$
$V_Y = 2.0$ V
OUTPUT VOLTAGE Vz
0
1
2

E. TEST 9

i. Purpose

To investigate the Texas Instrument TL 441 log amplifier.

ii. Log Configuration

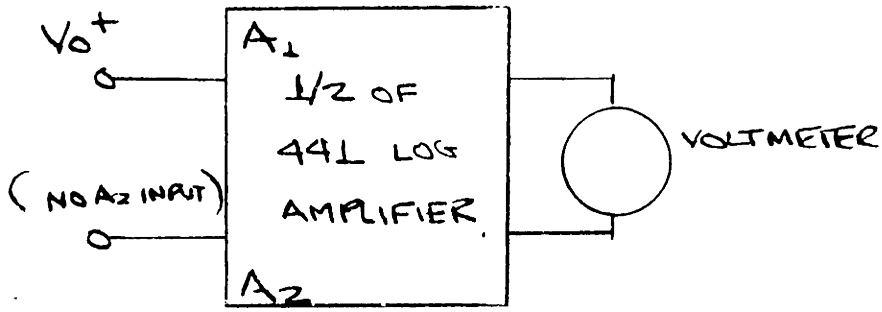

V_o	$V_{y\bar{y}}$	V_o	$V_{y\bar{y}}$
.002	.028		
.010	.060		
.020	.097		
.030	.143		
.080	.251		
.100	.275		
.150	.313		
.200	.343		
.300	.379		
.500	.416		
1.003	.423		
2.00	.427		

(VIRTUALLY IDENTICAL FOR INPUT AT PIN A2)

The output characteristic $V_{Y\bar{Y}} = \Sigma \log A_1 + \log A_2$ verified. From the plot, "TL 441 transfer characteristics, the log amplifier has 1 1/2 decades of dynamic input range, from 20 - 600 mV.

iii. Antilog Configuration

TWO ALTERNATE WIRINGS WERE INVESTIGATED:

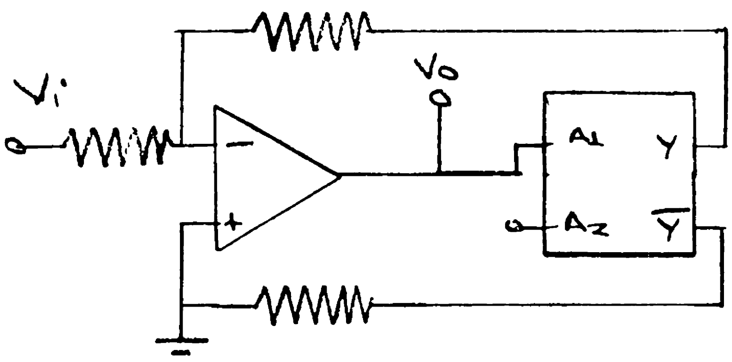

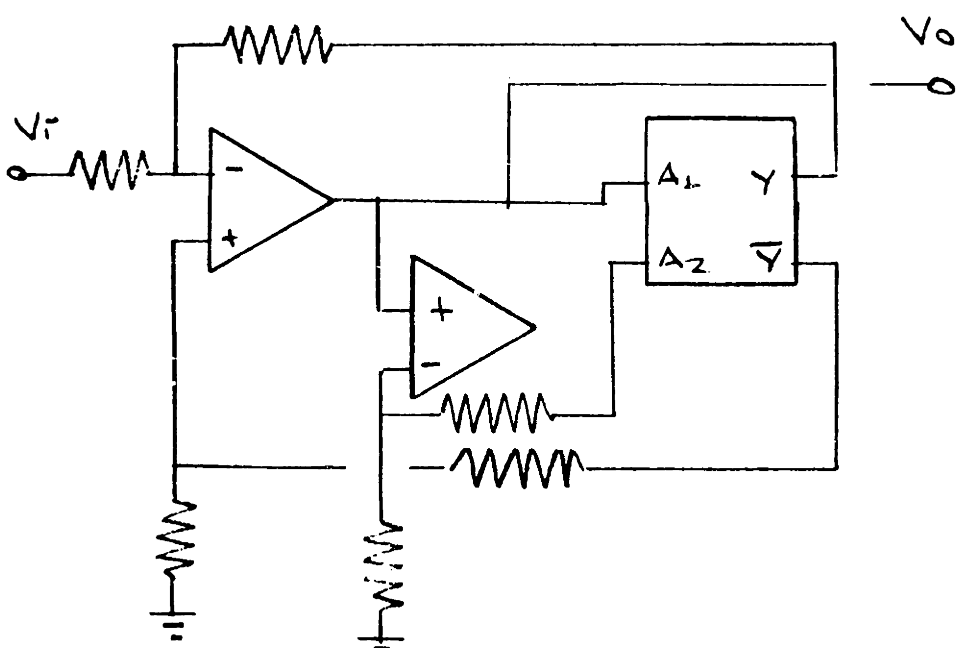

Antilog Configuration 1

V_i	V_o	$V_o + .028$
-.001	-.028	0
-.010	-.026	.002
-.049	-.018	.013
-.100	-.002	.050
-.200	.025	.053
-.300	.063	.091
-.400	.171	.199
-.500	.296	(.296) SATURATION
-.600	.296	
-.701	.296	
-.120		
-.150	NO DATA	
-.180		
-.350	.098	.126
-.450	.293	(.293) SATURATION
-.420	.213	.241

The antilog data is graphed in "TL 441 antilog characteristics" for configuration 1. Configuration 2 will expand the antilog dynamic range somewhat above the 1 1/2 decades available for configuration 1.

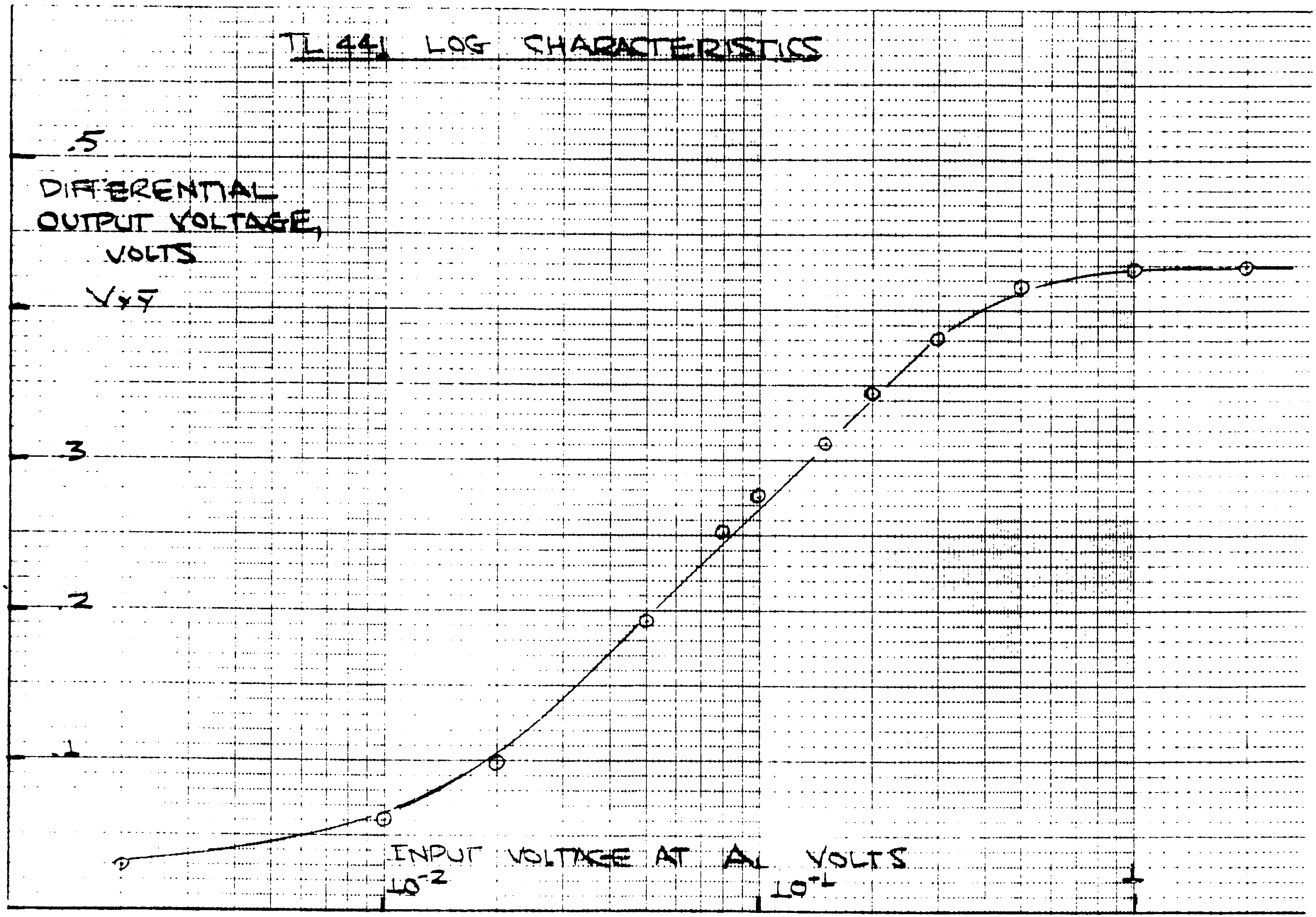
TL 441 LOG CHARACTERISTICS
.5
DIFFERENTIAL
OUTPUT VOLTAGE,
VOLTS
3
2
.1
INPUT VOLTAGE AT A1 VOLTS
10-2
10-1
1

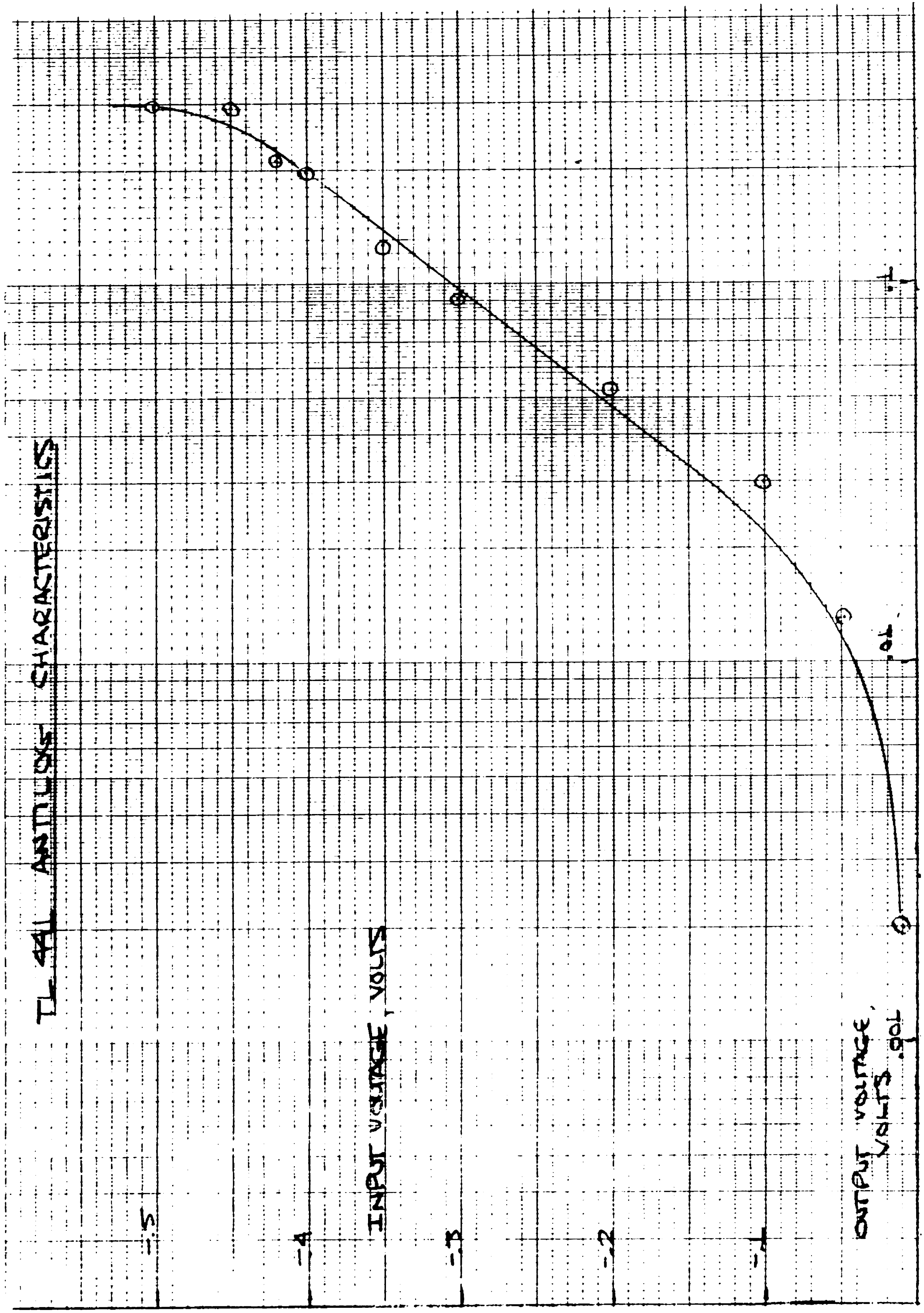
TL 441 ANTILOG CHARACTERISTICS
INPUT VOLTAGE, VOLTS
OUTPUT VOLTAGE, VOLTS
-.5
-.4
-.3
-.2
-.1
.001
.01
.1

F. TEST 10

i. Purpose

To incorporate the 441 log amplifier and the quadrant multiplier in the variable exponent circuit. The general wiring is sketched below:

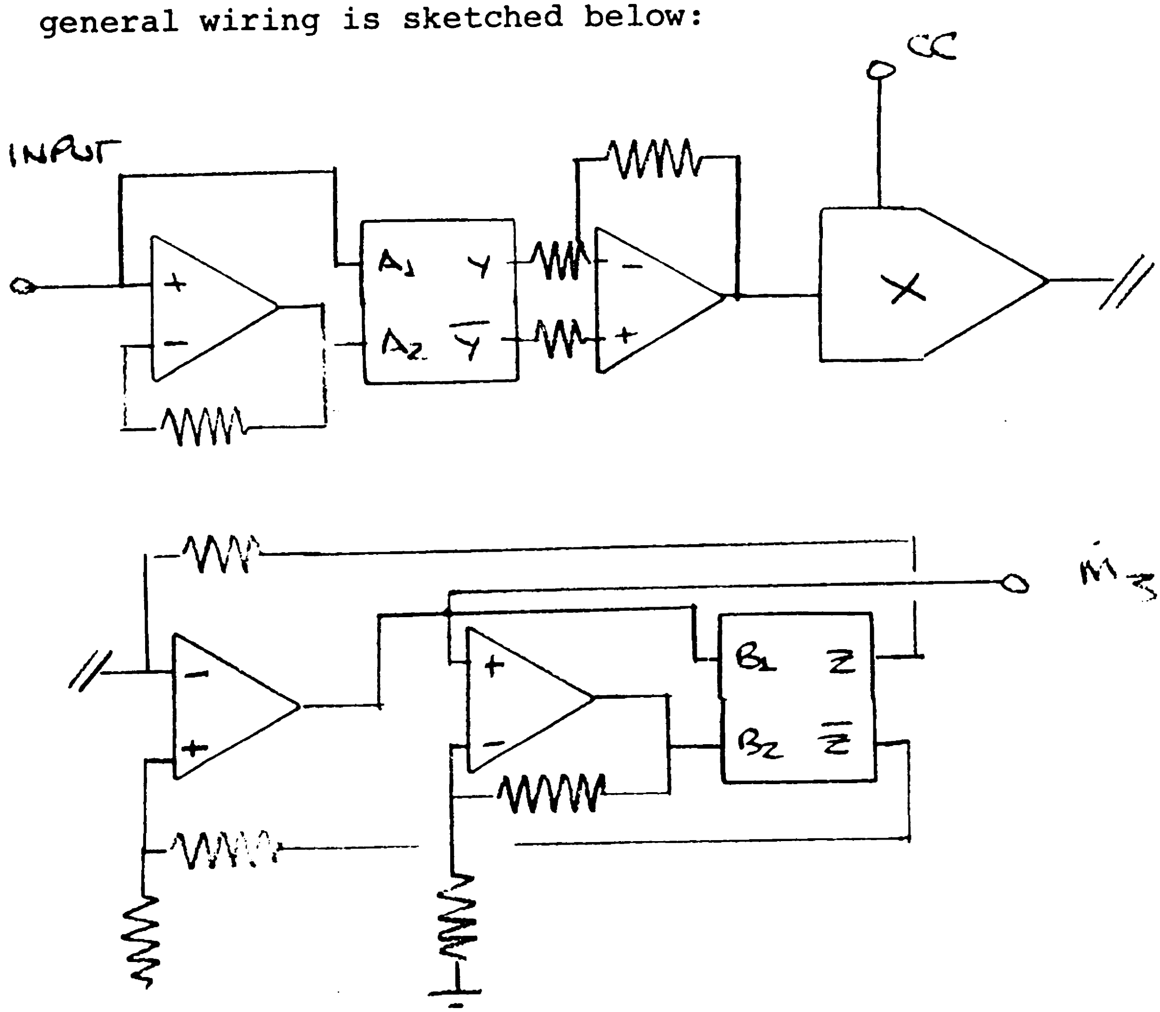

ii. Steady State Performance

The circuit demonstrated the ability to track a desired variable exponent. It was of primary interest to determine if the thermal properties were improved over the simple log-fed multiplier circuit.

The following data was generated:

Variable Exponent Test

1.50	1.39	1.45
1.57	1.47	1.37
1.55	1.47	1.46
1.47	1.42	1.41
1.55	1.47	1.33
1.52	1.54	1.41
1.45	1.45	1.43
1.52	1.41	
1.50	1.46	

(VOLTS)

25 Samples

MEAN = 1.474 VOLTS

STD DEVIATION = .052 VOLTS

This represents a 50% reduction in the drift over the simple log configuration. Since the 441 log amplifier is fairly cheap, it is substituted for the simple log configuration.

APPENDIX IV

DYSYS SIMULATION

```
      SUBROUTINE MOSIM
      COMMON T,DT, Y(20), F(20), STIME,FTIME,NEWDT,IFWRT,N
      REAL NG
      IF(NEWDT.NE.-1) GO TO 1
      GEC = .2831
      GET = .2536
    1 IF(NEWDT.EQ.0) GO TO 2
      P3 = Y(1)
      T4 = Y(2)
      NG = Y(3)
      Y(5) = P3/16328.
      Y(6) = T4/2159.
      Y(7) = NG/8000.
      PRC = P3/2041.2
      PRT = 1./PRC
      YNC = NG/7200.
      YNT = NG/(SQRT(T4)*172.62)
      AC = .75*XNC+.27*XNC**3.0
      BC = 3.*YNC**1.5 + 3.*XNC**7.
      CC = .01803*(2.-XNC)**5.794
      DC = .8906*SQRT(.9-(XNC-.9)*(XNC-.9))
      FC = 3.
      EC = 1. + YNC+ 3.6*YNC**4.1
      XWC = AC*(1.-(PRC-1.)/BC)**CC
      EFFC = DC*(1.-((EC-PRC)/(EC-1.))**FC)
      TRC = 1. +(PRC**GEC-1.)/EFFC
      AT = 1.0006
      BT = 3.1 + 1.62/(YNT + .26)
      CT = .7
      TT = .88*(1.-(1.-XNT)**4.)**.65
      ET= 1.-.8*YNT**1.25
      YWT = AT*(1.-PRT**BT)**CT
      EFFT = TT*(1.-(1.-SQRT((1.-ET)/(1.-PRT)))*(1.-SQRT((1.-ET)/(1.-
     1PRT))))
      TRT = 1.-EFFT*(1.-PRT**GET)
      WC = 100.*YWC
```

```
      TC = 539.69*TPC
      WT = .4086*P3/SQRT(T4)
      TE = T4*TRT
      TOC = 1798.*WC*(TC-539.)/NG
      TQT = 2011.*WT*(T4-TE)/NG
      IF(T.LT.FTIME-1.) GO TO 2
      PUT PPC,PRT,XNC,XNT,AC,BC,CC,DC,EC,XWC,FFFC,TPC,AT,BT,CT,TT,ET,
     1XWT,FFFT,TRT,WC,TC,WT,TE,TOC,TQT
    2 F(1) =800.*(WC-WT)
      F(2) = .0684*(WC*TC+70225.*Y(4)-WT*Y(2))
      F(3) = .3391*(TQT-TOC-.000097*Y(3)**2.)
      END


      DYSYS SYSTEM NAMELIST
          STIME = 0., FTIME = 10.,  TSTEP = .05, N = 3,
          Y(1) = 10206., Y(2) = 1739.7, Y(3) = 7200., Y(4) = 1.1807
    IPRNT=1,2,3,  PRNTC=9., 10., 1.8
```

```
XNT    =  1.0007      AC    =  1.0212
FC     =  5.6120      YWC   =  1.0013
RT     =  4.3850      CT    = 0.70000
FFFT   = 0.88000      TPT   = 0.70487
TF     =  1226.3      TOC   =  9312.9
PRC    =  5.0076      PRT   = 0.19970         XNC   =  1.0008
BC     =  6.0194      CC    = 1.79508E-02     DC    = 0.84012
EFFC   = 0.83823      TRC   =  1.6894         AT    =  1.0006
TI     = 0.88000      ET    = 0.19926         XWT   =  1.0000
WC     =  100.13      TC    =  911.73         WT    =  100.13
TOT    =  14349.
10.00     5.0000E-02  1.0221E 04   1740.         7205.

EXTREME VALUES OF STATE AND AUXIITARY VARIABLES
                   MINIMUM            MAXIMUM
  Y( 1)          1.0206E 04         1.0221E 04
  Y( 2)           1740.              1741.
  Y( 3)           7200.              7205.
  Y( 4)           1.181              1.181
  Y( 5)          0.6250             0.6260
  Y( 6)          0.8058             0.8062
```

APPENDIX V

DESIGN DRAWINGS AND SKETCHES

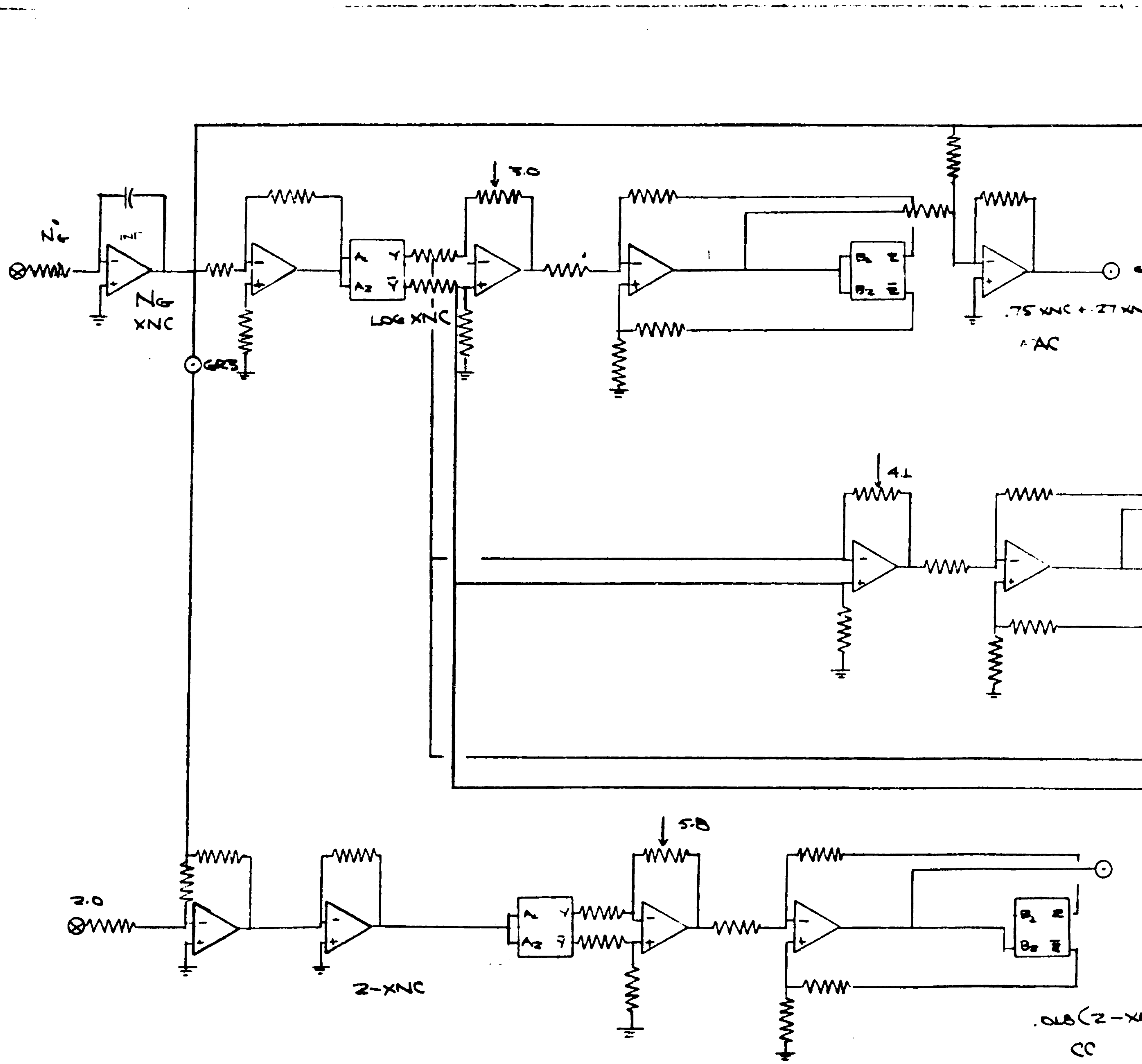
Ṅ_G
N_G
XNC
GRS
LOG XNC
.75 XNC + .27 XN
AC
4.1
2.0
2-XNC
5.8
CC

GRID 1

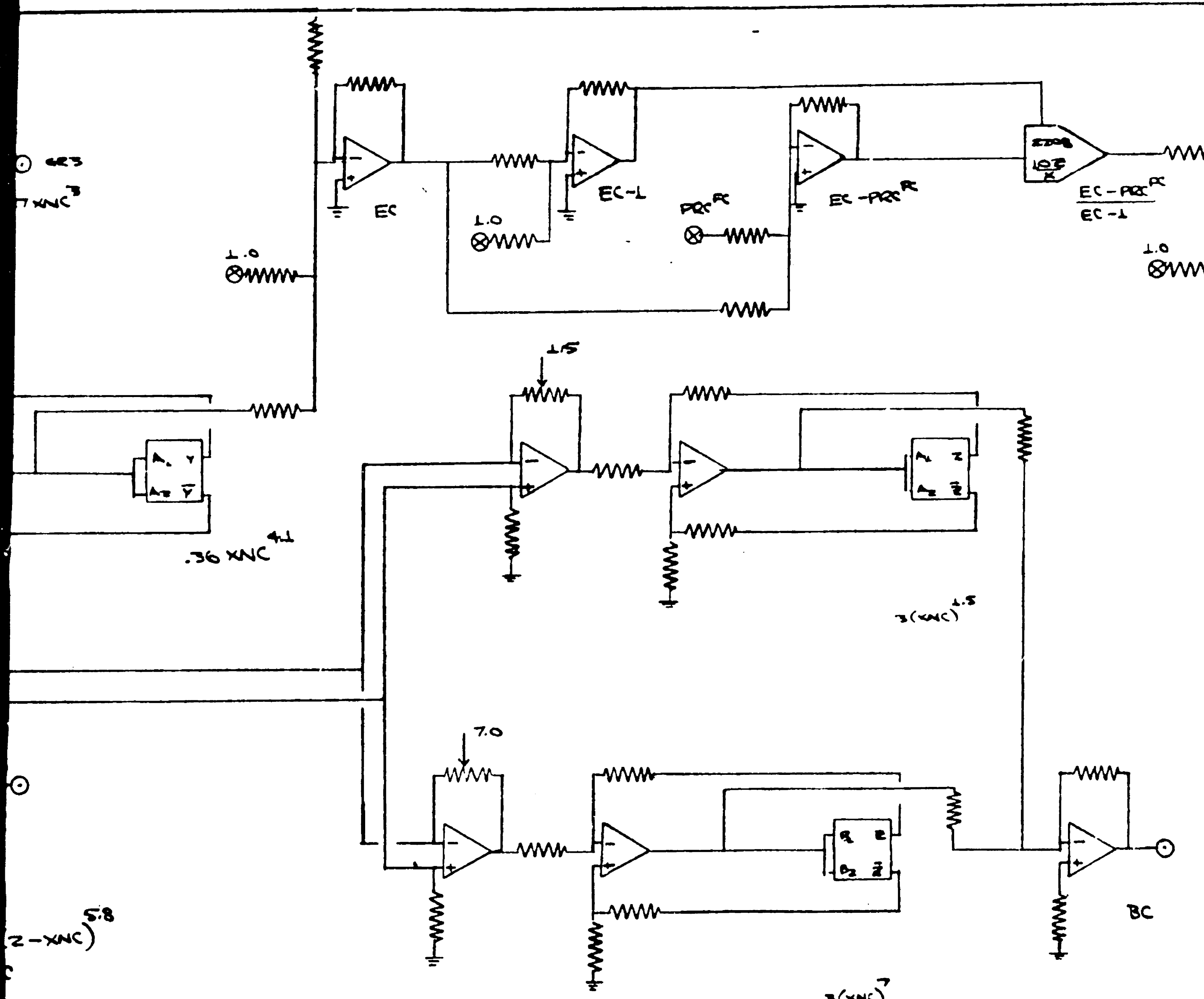

GR3
EC
EC-1
1.0
PRC^PC
EC-PRC^PC
EC-PRC^PC / EC-1
1.0
1.0
1.5
.36 XNC^4.1
3(XNC)^1.5
7.0
BC
(Z-XNC)^5.8
3(XNC)^7

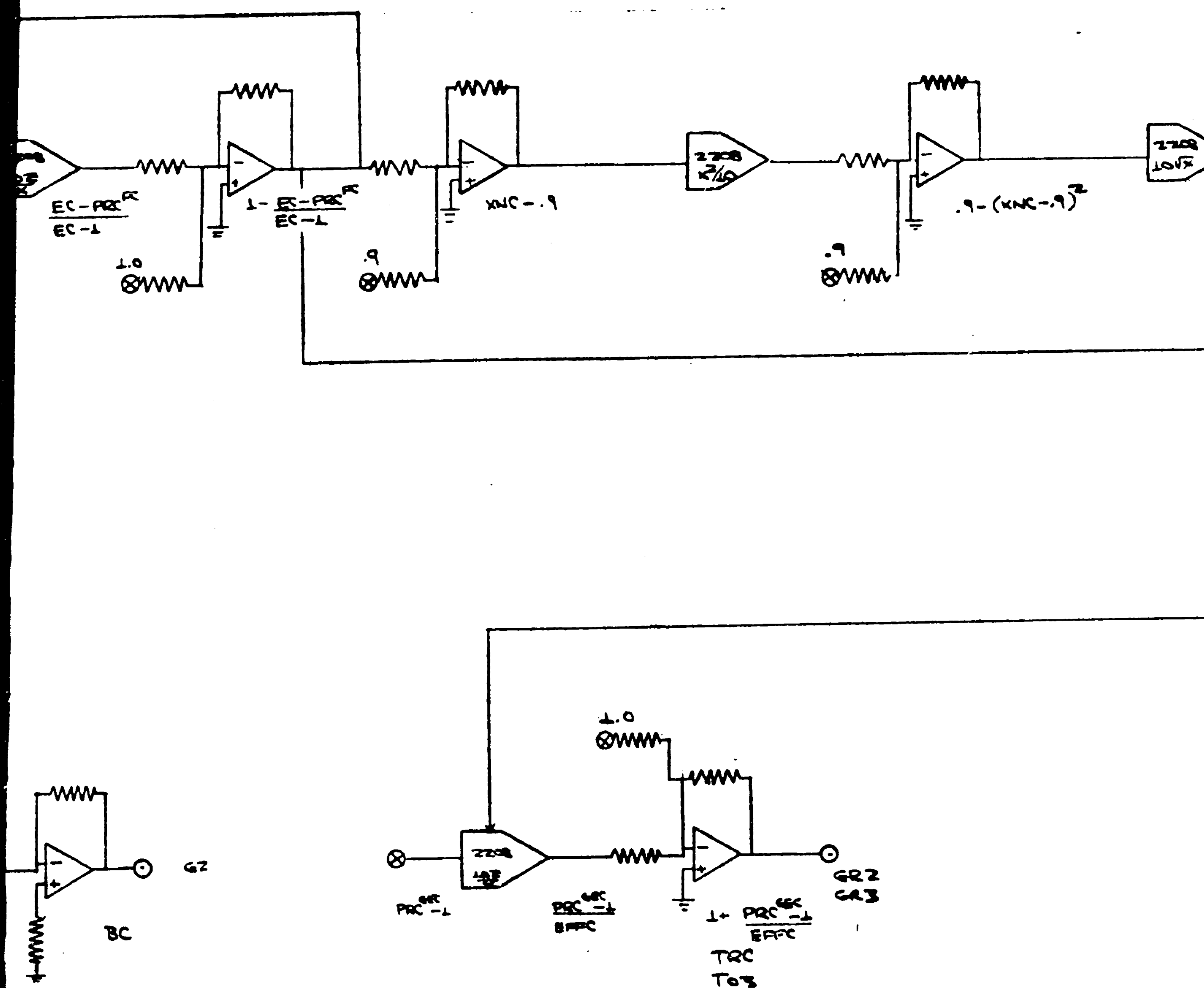
EC - PRC^FC / EC - 1
1 - EC - PRC^FC / EC - 1
1.0
.9
XNC - .9
2208
X²/10
.9 - (XNC - .9)²
.9
2208
10√X
G2
BC
1.0
2208
PRC^GEC - 1
PRC^GEC - 1 / EFFC
1 + PRC^GEC - 1 / EFFC
GR2
GR3
TRC
T03

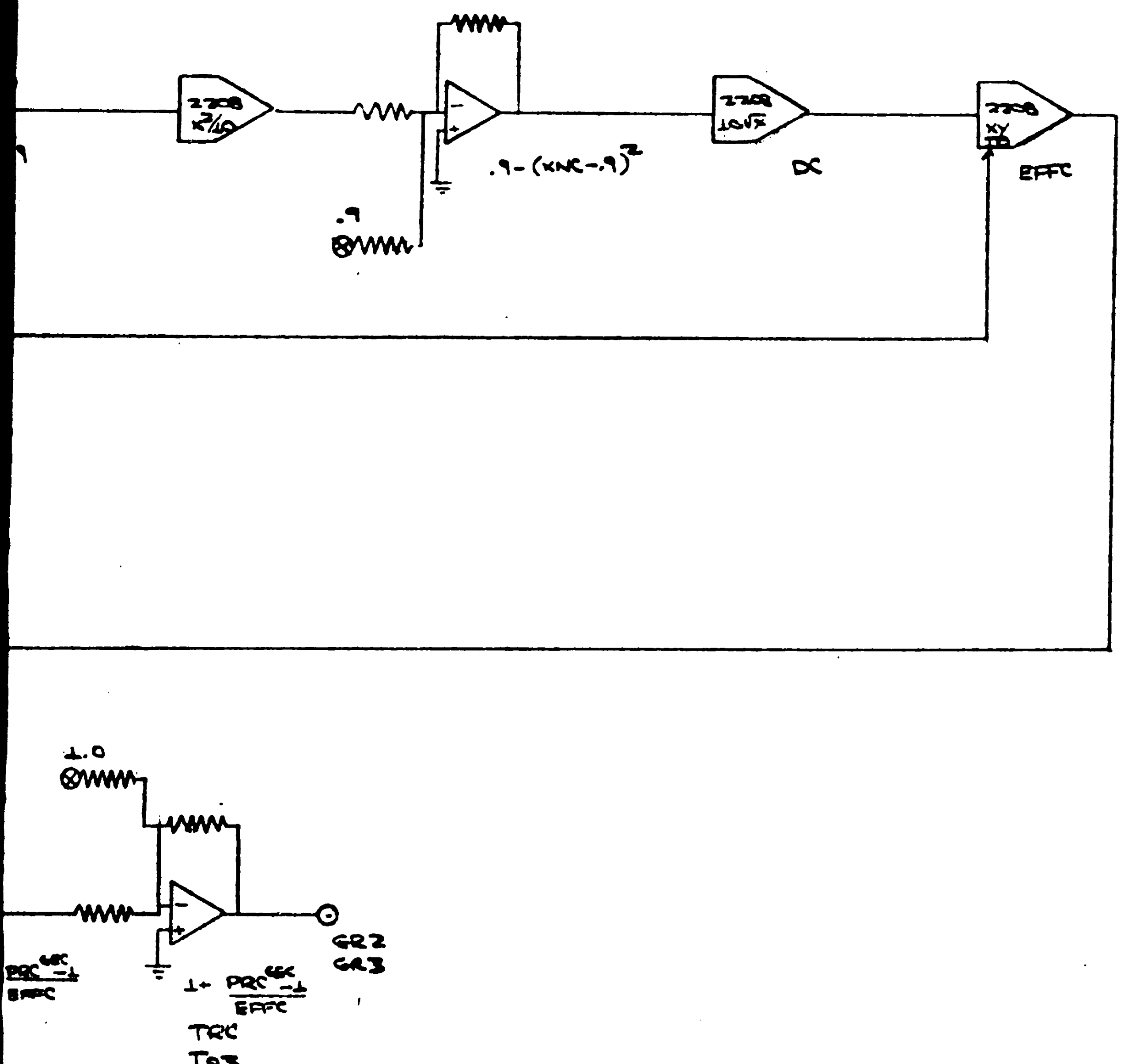

2208
.9
.9-(XNC-.9)²
2208
DC
2208
XY
EFFC
1.0
GR2
GR3
TRC
T03

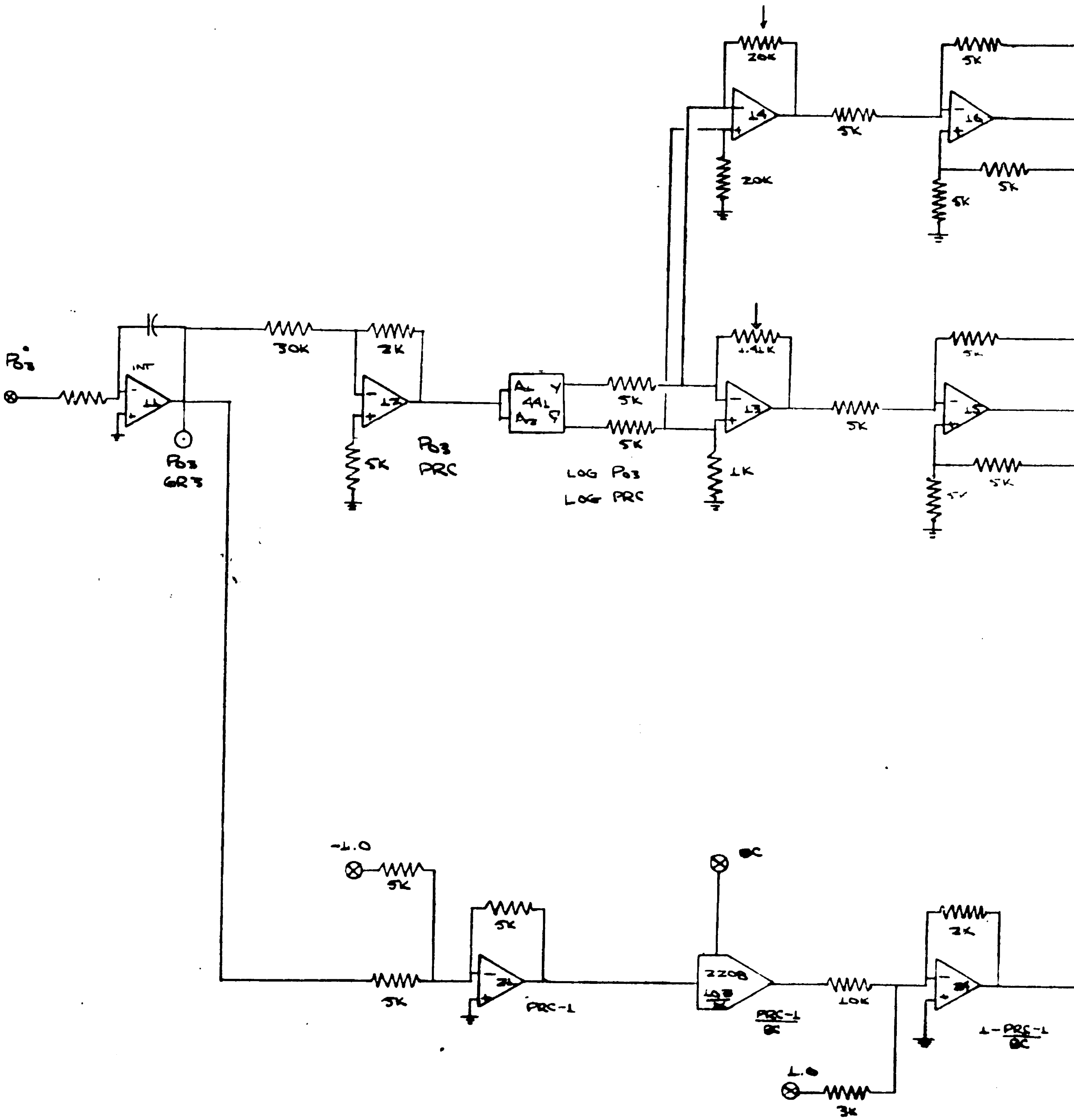
INT
30K
2K
5K
441
5K
5K
LOG
PRC
20K
20K
5K
5K
5K
5K
1.41K
1K
5K
5K
-1.0
5K
5K
5K
PRC-1
2208
10K
3K
1.0
2K

GRID Z

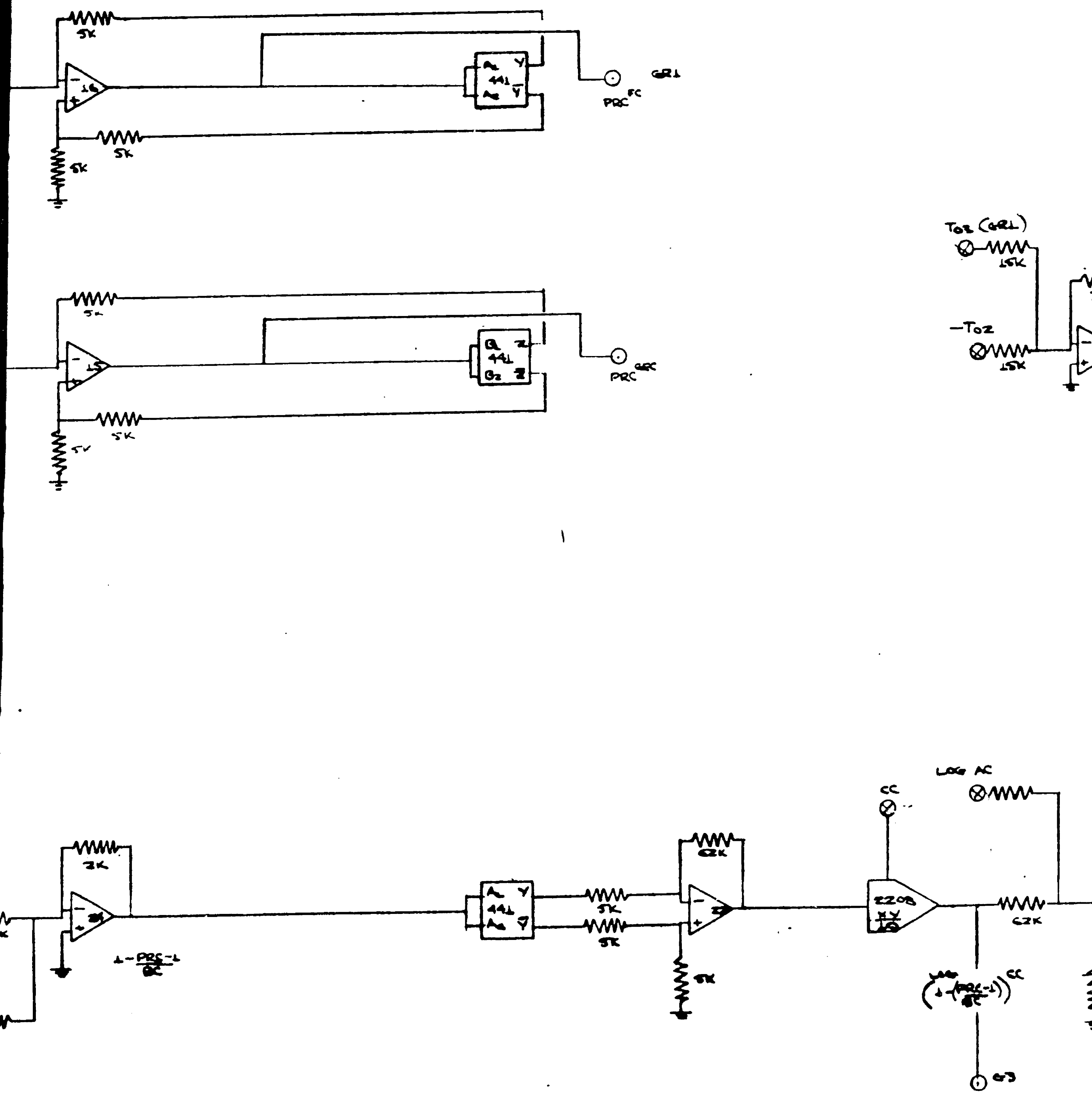

5K
441
PRC FC
GR1
5K
5K
441
PRC GRC
5K
5K
To2 (GR1)
15K
-To2
15K
2K
441
5K
5K
62K
5K
2208
LOG AC
CC
62K
G3

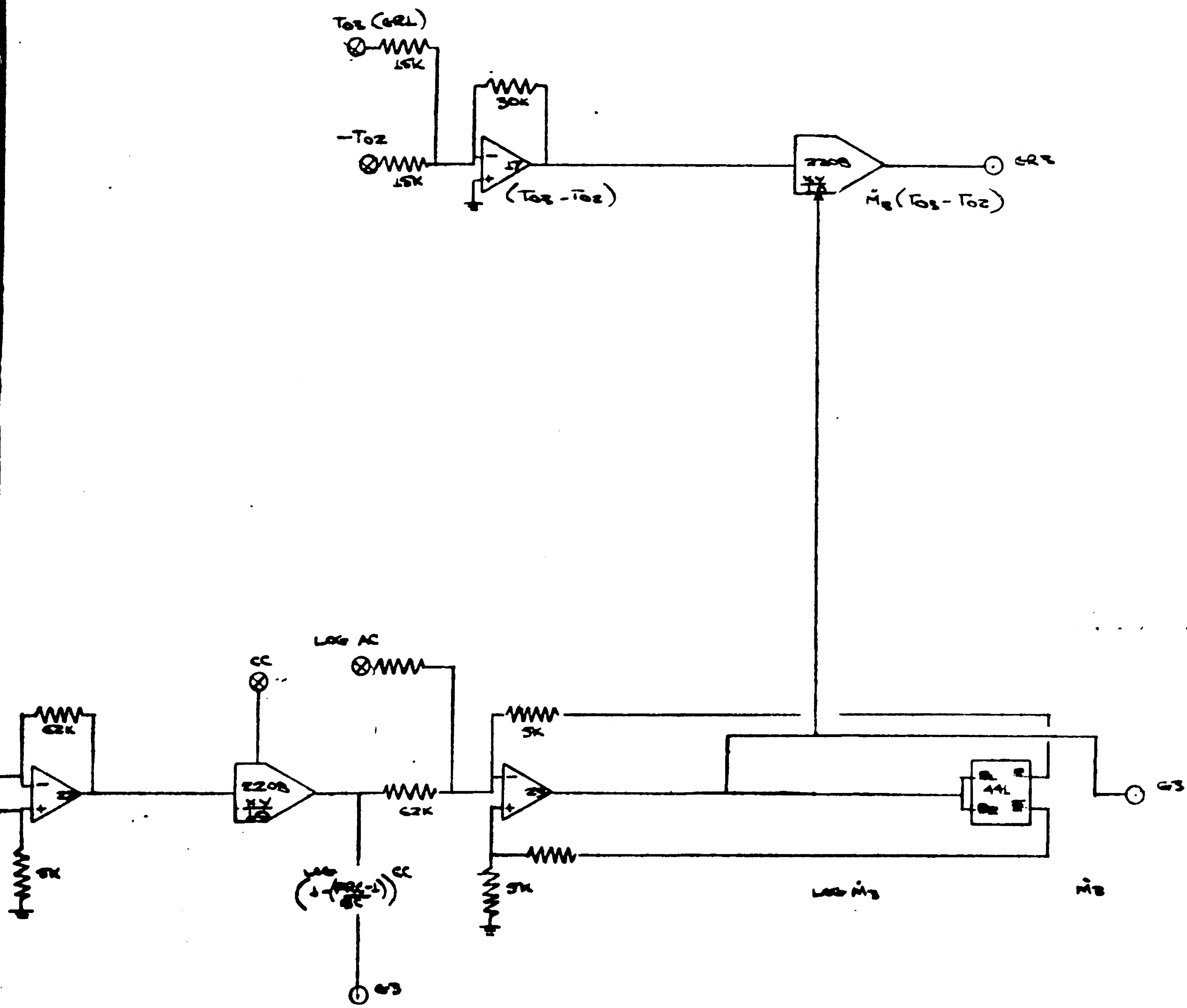

15K
30K
−T02
15K
LOG AC
CC
62K
5K
62K
5K
5K
441
LOG

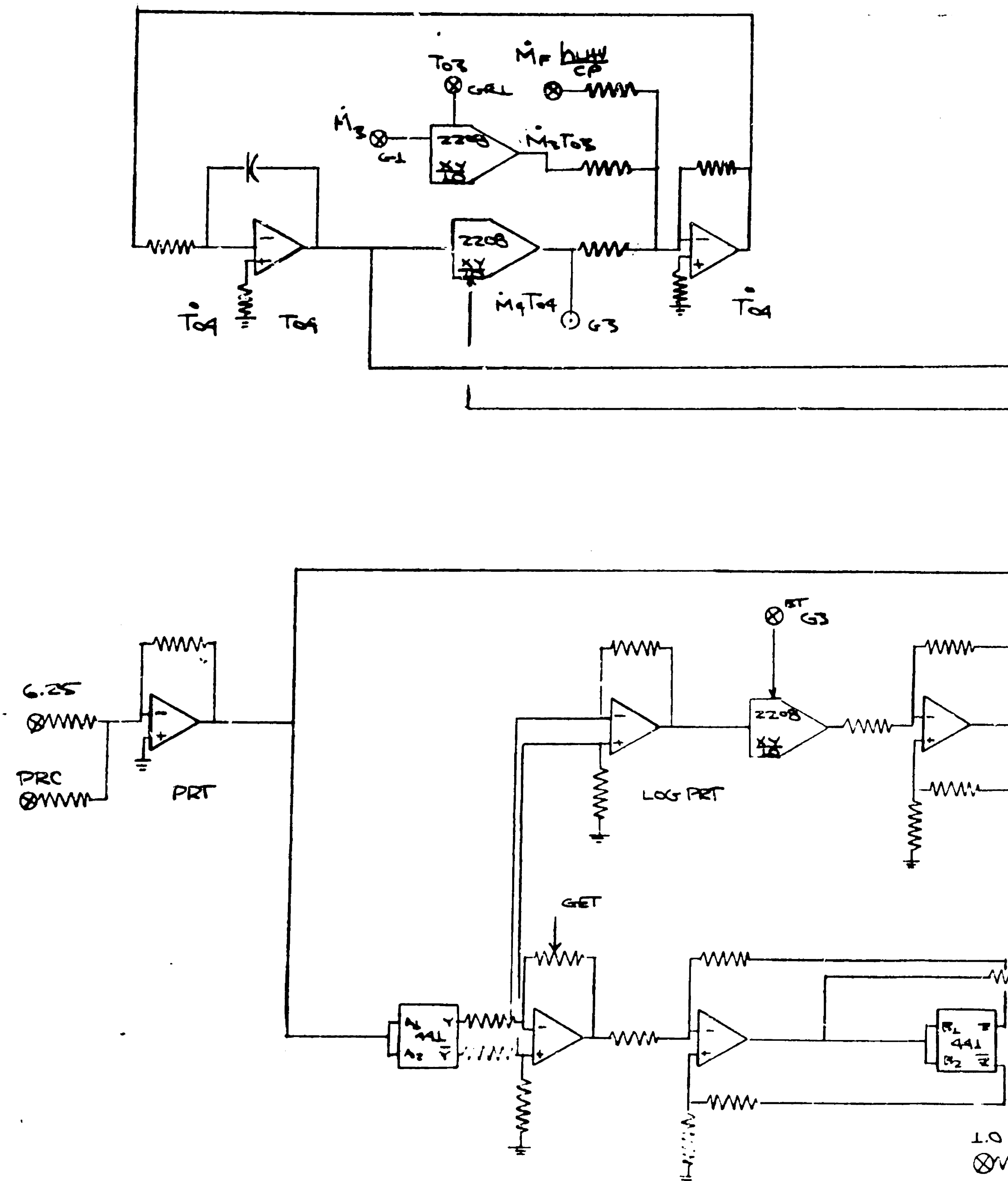
2208
XY/10
2208
XY/10
G3
2208
XY/10
LOG PRT
PRT
PRC
6.25
GET
441
441
1.0

GRID 3

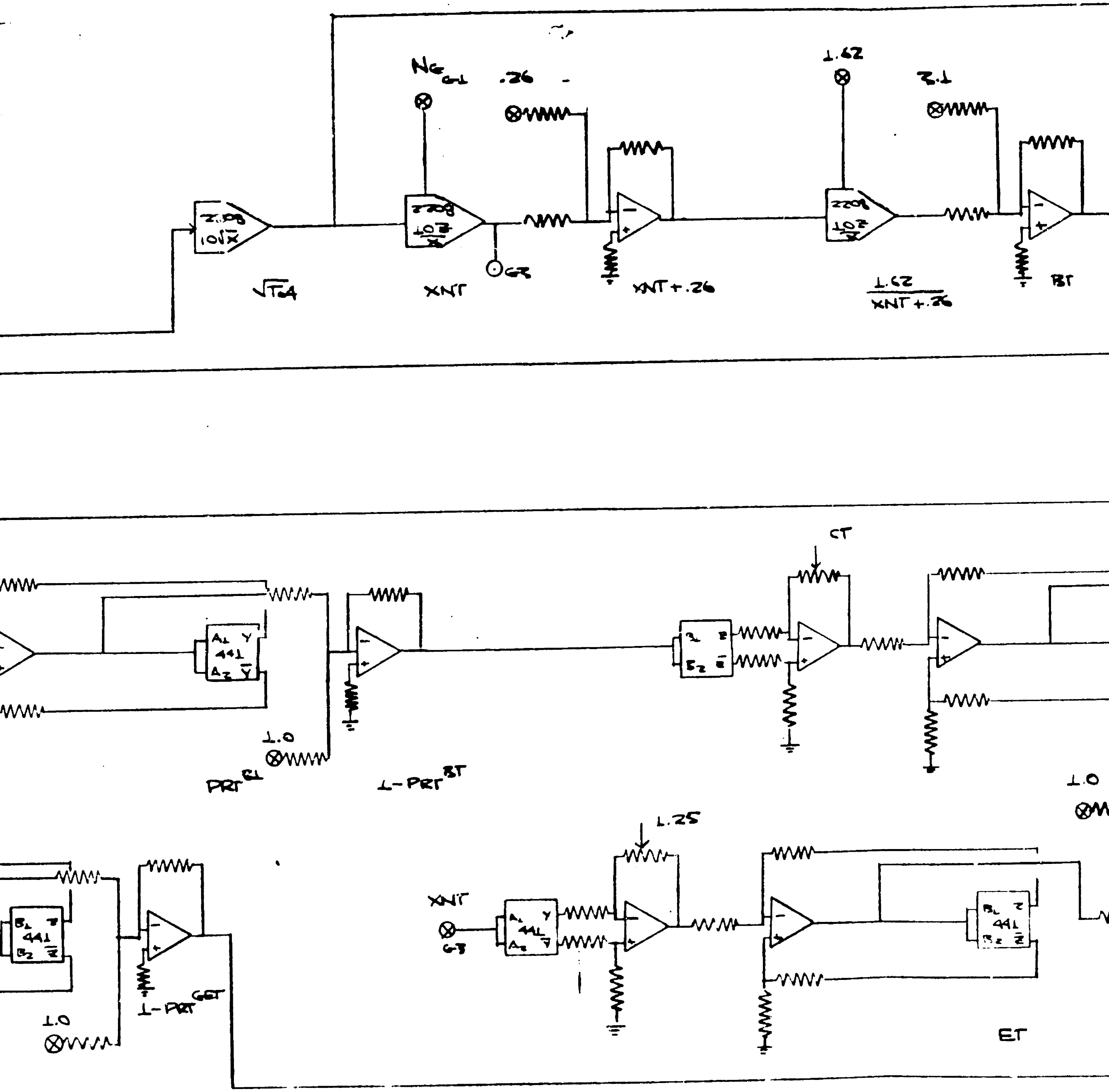

NG
.26
1.62
3.1
2.08
10√x
2208
10Z/X
√T64
XNT
GT
XNT+.26
1.62 / XNT+.26
BT
CT
441
1.0
PRT
1-PRT
1.25
XNT
GT
ET
1-PRT

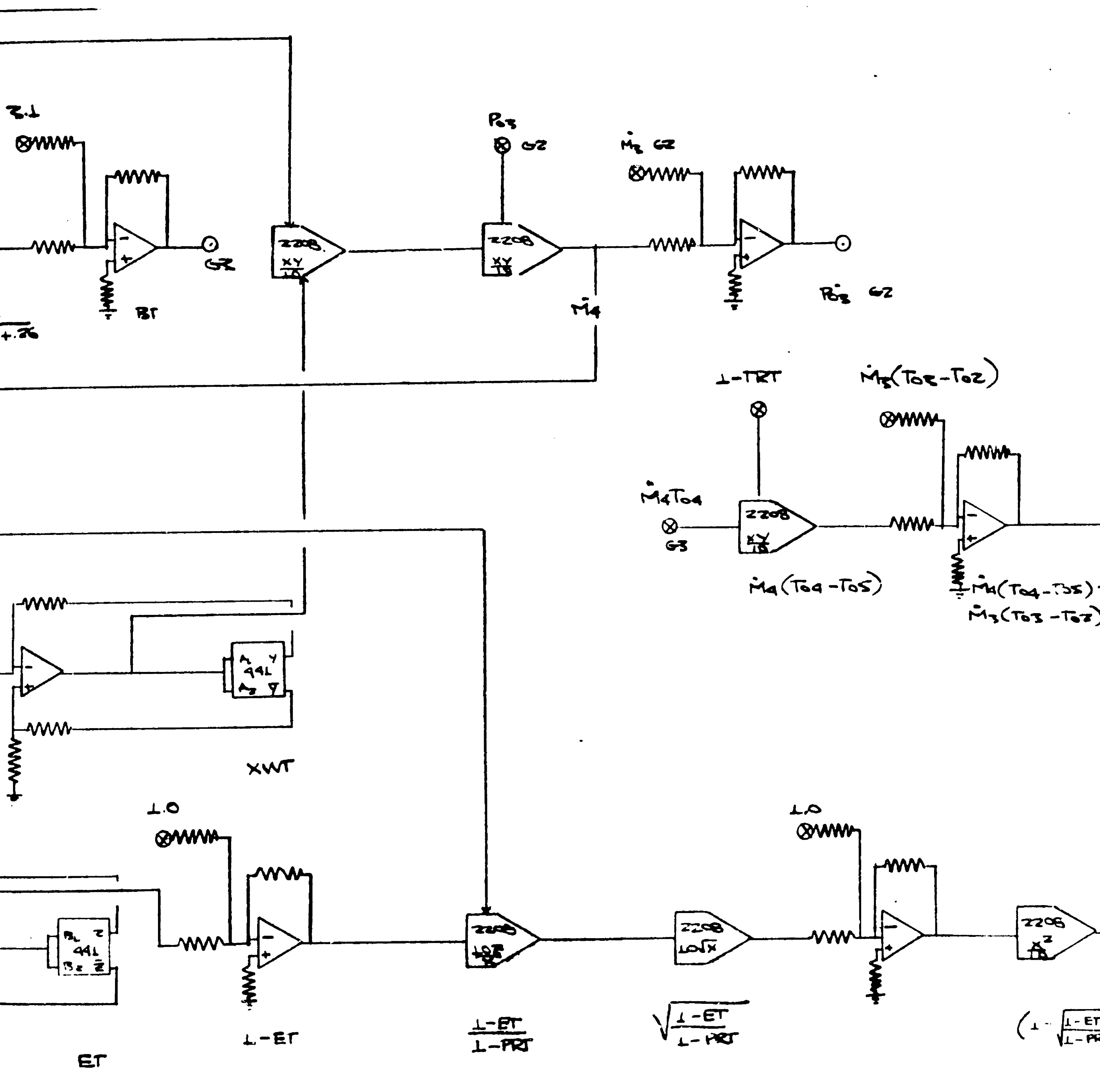

Pₒ₃ G2
Ṁ₃ G2
2208 XY
2208 XY
G2
BT
Ṁ4
Pₒ₃ G2
1-TRT
Ṁ₃(To3-To2)
Ṁ4To4
G3
2208 XY
Ṁ4(To4-To5)
Ṁ4(To4-T35)
Ṁ3(To3-To2)
441
XWT
1.0
1.0
441
2208
2208
2208
1-ET
1-ET / 1-PRT
√(1-ET / 1-PRT)
ET

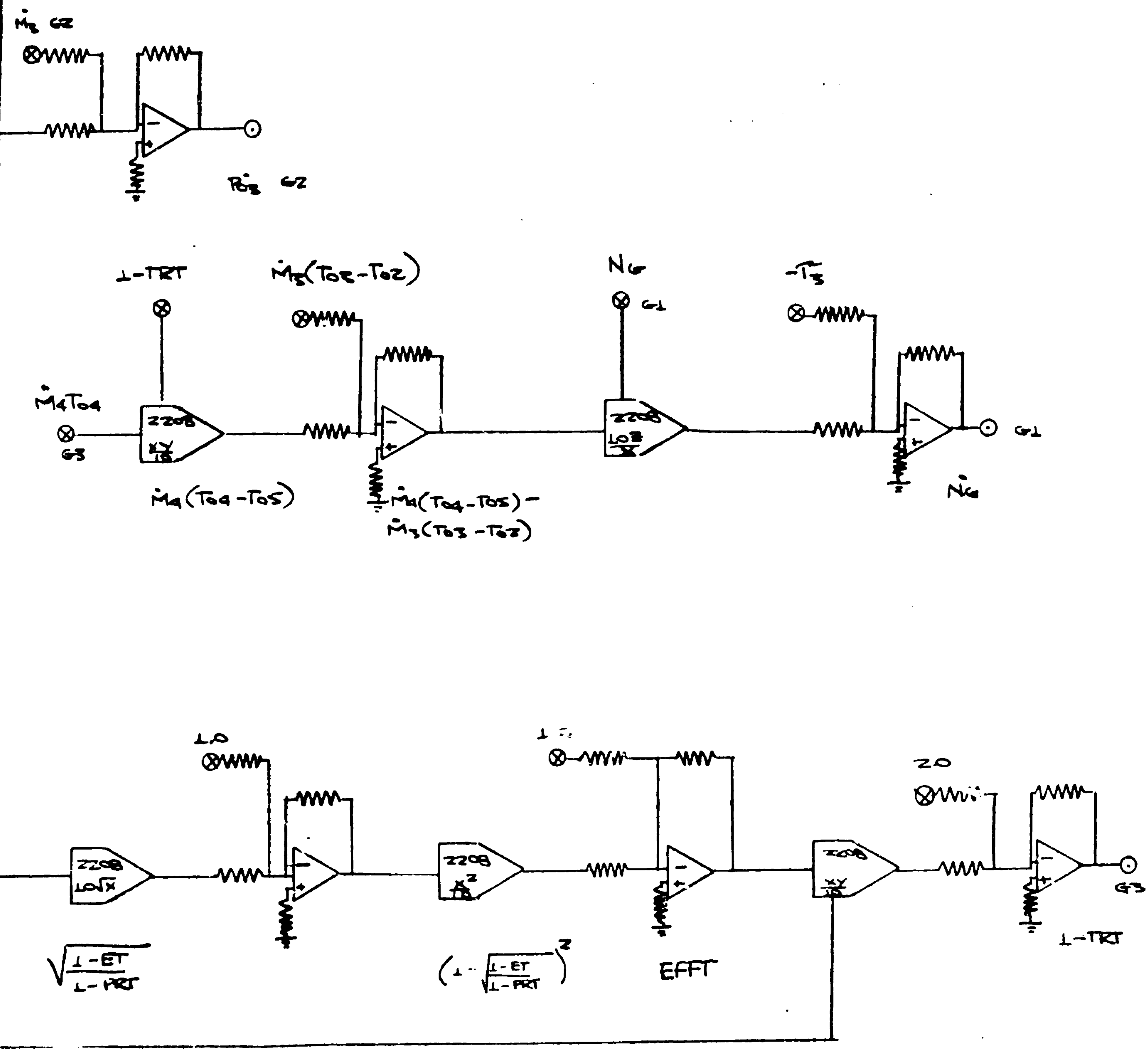

M3 G2
P03 G2
1-TRT
M3(To3-To2)
M4To4
G3
2208
XY/10
M4(To4-To5)
M4(To4-To5)-
M3(To3-To2)
NG
G1
2208
-T3
G1
NG
1.0
2208
10√X
√((1-ET)/(1-PRT))
2208
X²/10
(1-√((1-ET)/(1-PRT)))²
EFFT
20
2208
XY/10
G3
1-TRT

SIMULATOR LAYOUT

(NOT TO SCALE)

EXTERIOR

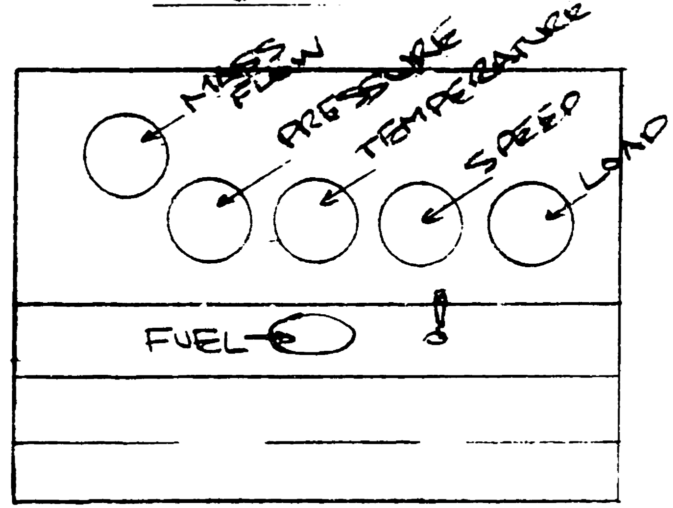

FRONT VIEW

INTERIOR

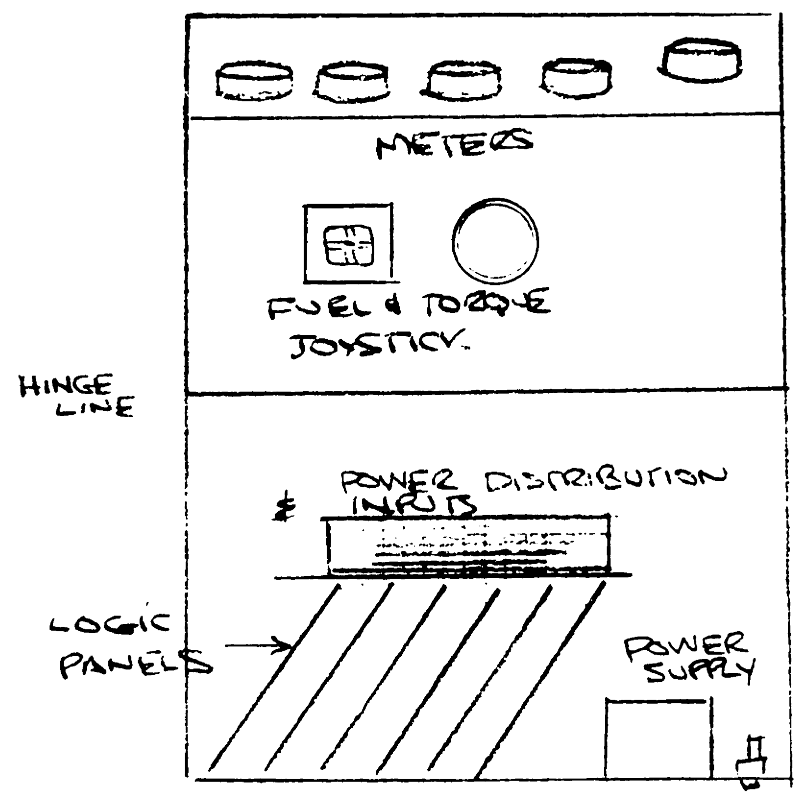

TOP VIEW

APPENDIX VI

SPECIFICATIONS

A. ELECTRONIC COMPONENTS

1. Operational Amplifiers

a. Fairchild μA 741

Maximum ratings supply voltage	± 18v
Power dissipation	500 MW
Supply current	2.8 MA
Typical input offset voltage	1 mv

b. Fairchild μA 324 Quad OP amp

Maximum ratings supply voltage single polarity	32v
Input voltage range	-0.3v to 32v
Power dissipation	900 MW
Supply current	2 MA
Typical input offset voltage	2 mv

2. EXAR 2208 Four Quadrant Multiplier

Maximum ratings supply voltage	± 18v
Power dissipation	750 MW
Typical supply current	5 MA
Typical output nonlinearity	.5%

3. <u>Texas Instruments TL 441 Logarithmic Amplifier</u>

Maximum ratings supply voltage	± 8v
Input voltage	6v
Power dissipation	500 MW
Typical differential output offset voltage	40 Mv
Typical supply current vcc^+	18.5 MA
vcc^-	8.5 MA

4. <u>Trimming Potentiometers</u>

All applications: Spectrol type 64 ceramic potentiometers, 1-100KΩ

5. <u>Resistors</u>

All applications: Corning 2% 1/4 watt resistors

6. <u>Power Supply</u>

Analog Devices model 975 dual polarity power supply

Output voltage	± 15v
Maximum rating	500 MA
Typical output error	1%

B. <u>PERIPHERALS</u>

1. <u>Breadboard Panels</u>

Continentíal Specialties model QT 59 6.5" panels

2. Volt Meters

Beede Instrument 3" panel meters, model 3-03-8

250° movement

200Ω internal resistance

3. Joystick

2 - axis movement; two, 100KΩ rotary potentiometers on each axis.

4. Chassis

.062" clear anodized aluminum assembled with pop-rivet construction.